Journal of Medicinal Chemistry

Article

Identification of GZD824 as an orally bioavailable inhibitor that targets phosphorylated and non-phosphorylated Bcr-Abl and overcomes clinically acquired mutation-induced resistance against imatinib

Ke Ding, Xiaomei Ren, zhang zhang, Xiaofeng pan, Zhengchao Tu, Xiaoyun Lu, Yupeng Li, Wang Deping, Donghai Wen, Huoyou Long, Jinfeng Luo, Yubing Feng, Xiaoxi Zhuang, Fengxiang Zhang, Jianqi Liu, Fang Leng, Xingfen lang, Yang Bai, Miaoqin She, and Jingxuan Pan

J. Med. Chem., **Just Accepted Manuscript** • DOI: 10.1021/jm301581y • Publication Date (Web): 09 Jan 2013

Journal of Medicinal Chemistry is published by the American Chemical Society. 1155 Sixteenth Street N.W., Washington, DC 20036

Identification of GZD824 as an Orally Bioavailable Inhibitor that Targets Phosphorylated and Non-phosphorylated Breakpoint Cluster Region-Abelson (Bcr-Abl) Kinase and Overcomes Clinically Acquired Mutation-Induced Resistance against Imatinib

Xiaomei Ren, [α, β, δ] *Xiaofen Pan,* [α, δ] *Zhang Zhang,* [α, δ] *Deping Wang,* [α, φ] *Xiaoyun Lu,* [α] *Yupeng Li,* [α, φ] *Donghai Wen,* [α] *Huoyou Long,* [α] *Jinfeng Luo,* [α] *Yubing Feng,* [α] *Xiaoxi Zhuang,* [α] *Fengxiang Zhang,* [α] *Jianqi Liu,* [α] *Fang Leng,* [α] *Xingfen Lang,* [α] *Yang Bai,* [α] *Miaoqin She,* [α] *Zhengchao Tu,* [α] *Jingxuan Pan* [β] *and Ke Ding* [α *]

[α] Institute of Chemical Biology, Guangzhou Institutes of Biomedicine and Health, Chinese Academy of Sciences, #190 Kaiyuan Avenue, Guangzhou 510530, China

[β] Zhongshan Medical School, Sun Yat-Sen University, #74 2nd Zhongshan Road, Guangzhou 510080, China

[φ] Graduate University of Chinese Academy of Sciences, # 19 Yuquan Road, Beijing 100049, China

[δ] These authors contributed equally to this work.

*Corresponding author: Tel: +86-20-32015276. Fax: +86-20-32015299.

E-Mail: ding_ke@gibh.ac.cn

RECEIVED DATE (to be automatically inserted after your manuscript is accepted if required according to the journal that you are submitting your paper to)

ABSTRACT. The Bcr-Abl ^{T315I} mutation induced imatinib-resistance remains a major challenge for clinical management of chronic myelogenous leukemia (CML). Herein, we report GZD824 (**10a**) as a novel orally bioavailable inhibitor against a broad spectrum of Bcr-Abl mutants including T315I. It tightly bound to Bcr-Abl^{WT} and Bcr-Abl^{T315I} with K_d values of 0.32 and 0.71 nM, respectively, and strongly inhibited the kinase functions with nM IC_{50} values. The compound potently suppressed proliferation of Bcr-Abl-positive K562 and Ku812 human CML cells with IC_{50} values of 0.2 and 0.13 nM, respectively. It also displayed good oral bioavailability (48.7%), a reasonable half-life (10.6 hrs) and promising *in vivo* anti-tumor efficacy. It induced tumor regression in mouse xenograft tumor models driven by Bcr-Abl^{WT} or the mutants, and significantly improved the survival of mice bearing an allograft leukemia model with Ba/F3 cells harboring Bcr-Abl^{T315I}. GZD824 represents a promising lead candidate for development of Bcr-Abl inhibitors to overcome acquired imatinib-resistance.

KEYWORDS: chronic myeloid leukemia (CML), GZD824, Bcr-Abl, imatinib resistance, T315I mutation

INTRODUCTION

The Bcr-Abl inhibitor imatinib (**1**) has provided significant clinical benefit and become the first-line drug for conventional treatment of Philadelphia chromosome positive (Ph^+) chronic myeloid leukemia (CML). However, emerging acquired resistance to drug **1** has become a major challenge for clinical management of CML. [1-6] For imatinib-treated CML patients, the 2-year incidence of resistance reaches 80% in the blastic phase, 40-50% in the accelerated phase, and 8-10% in the chronic phase. The occurrence of point mutations in the Abl kinase domain is the primary mechanism underlying imatinib-resistance. [7-9] More than 100 resistance-related Bcr-Abl mutants have been identified in the clinic, among which the "gatekeeper" T315I is most common mutation, as it accounts for approximately

15~20% of all clinically acquired mutants. Great efforts have been devoted to identifying novel Bcr-Abl inhibitors to overcome imatinib resistance. Nilotinib (**2**) [10], dasatinib (**3**) [11] and bosutinib [13] have been approved as second-line drugs to treat adult patients in all phases of CML with resistance to drug **1**. Many other inhibitors, such as bafetinib, [12] have also been developed in late-stage clinical trials (Figure **1**). However, the second-generation inhibitors are not capable of inhibiting the most refractory Bcr-Abl ^{T315I} mutant. [14-16] Bcr-Abl ^{T315I}-induced drug resistance remains an unmet clinical challenge for CML treatment.

T315 is one of the most critical residues for the binding of type I and type II inhibitors in the ATP-binding pocket of Bcr-Abl kinase. [17, 18] The T315I mutation disfavors a key hydrogen bonding interaction between the classical Bcr-Abl inhibitors and the kinase, whereas the bulky isoleucine side chain of I315 prevents the inhibitors from accessing an important hydrophobic pocket at the back of the ATP-binding domain. Moreover, the T315I mutation is also associated with a conformational change of the kinase from DFG-out to DFG-in, which further disrupts the binding of type II inhibitors to the Abl kinase domain. [19-22] In addition to a mutation in the kinase gatekeeper region (T315I/A), various mutations in the p-loop region (i.e., G250E, Q252H, Y253H, and E255K/V) and the hinge region (F317L/V) that confer imatinib resistance have also been identified. Notably, the inhibitory activity of **2** and **3** against the p-loop (Y253H and E255K/V) and the hinge of Bcr-Abl mutants (F317V), respectively**,** has been reported to be relatively limited. [23, 24, 25]

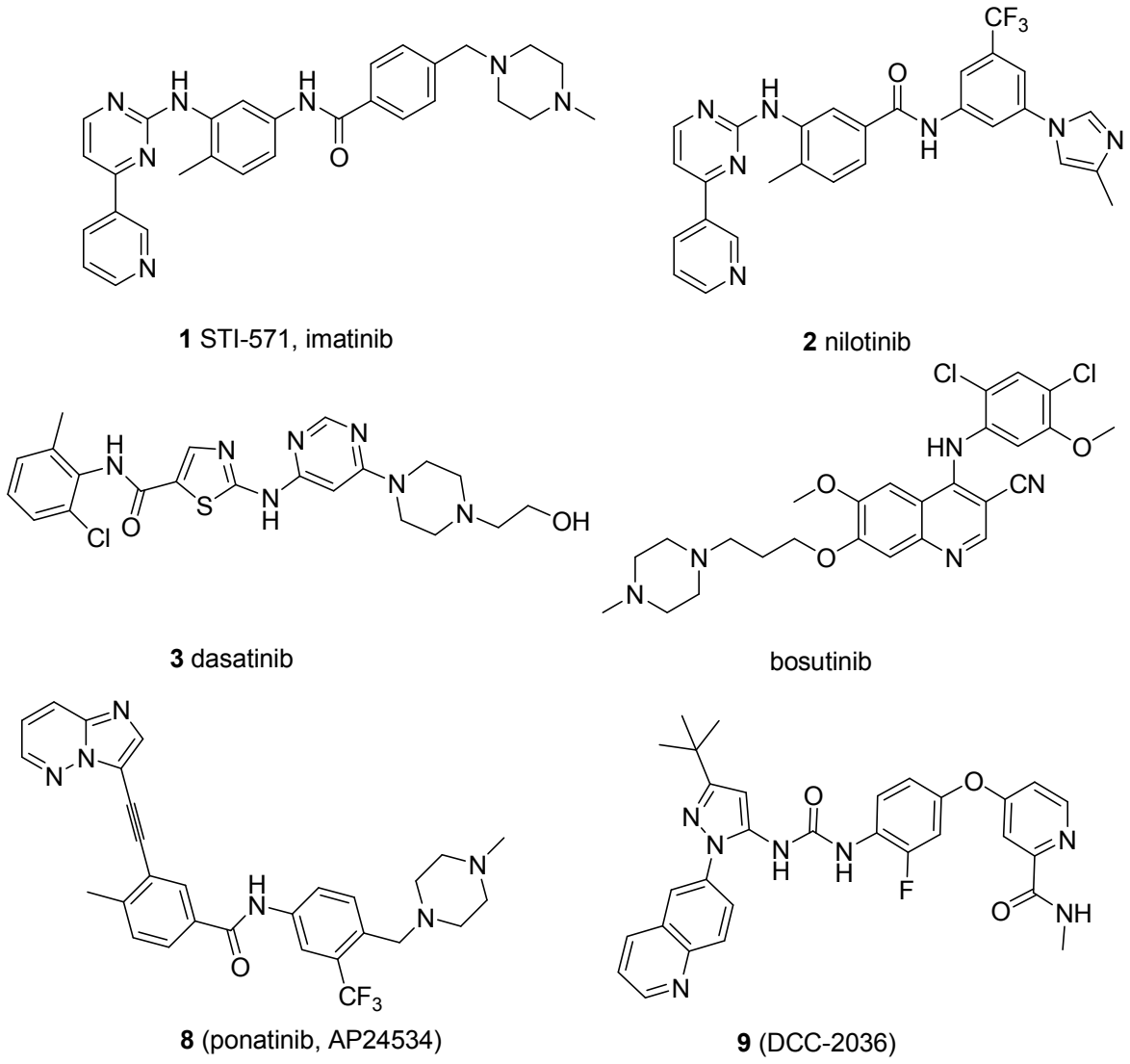

Figure 1. Chemical structures of FDA-approved and newly developed Bcr-Abl inhibitors.

Several small molecules capable of inhibiting the Bcr-Abl ^{T315I} mutant in biochemical and cellular assays have been reported.[26] Examples include the type I inhibitor PPY-A, c-Src/Abl dual inhibitor TG100598 and non-ATP-competitive or allosteric inhibitors (ON012380 or GNF-2, respectively). Several ATP-competitive Aurora kinase inhibitors, such as MK-0457 (**4**) [27], PHA-739358 (**5**) [28], AT9283 (**6**) [29] and XL-228 (**7**), [30] have been reported to inhibit Bcr-Abl ^{T315I}. However, most of these compounds appear to lack oral bioavailability, as they were formulated for intravenous administration. Furthermore, the clinical development of compound **4** has been discontinued because of its toxicity. Although **6** potently inhibits the activity of the Bcr-Abl ^{T315I} mutant and Bcr-Abl variants with

mutations in the p-loop and hinge regions, the mechanism underlying this broad spectrum of inhibition and the relative selectivity of this compound for Bcr-Abl over other off-target kinases require further investigation. As imatinib-resistant mutants are increasingly observed in the clinic, next-generation "pan-Bcr-Abl inhibitors" are required to not only overcome T315I resistance but also display broad inhibitory activity towards multiple Bcr-Abl mutants. [31-33] Recently, several "third-generation" Bcr-Abl inhibitors capable of inhibiting nearly the full range of Bcr-Abl kinase domain mutants in addition to the native enzyme were disclosed, among which AP24534 (**8**) [34] and DCC2036 (**9**) [35] are under clinical investigation.

Herein, we report the identification of GZD824 (**10a**) as a new orally bioavailable pan Bcr-Abl inhibitor with potency against a wide range of Bcr-Abl mutants, including the highly refractory gatekeeper mutant Bcr-Abl ^{T315I}; p-loop region mutants Bcr-Abl ^{G250E}, Bcr-Abl ^{Q252H} and Bcr-Abl ^{E255K}; and the ATP-binding domain hinge region mutant Bcr-Abl ^{F317L}, in addition to the native enzyme. Furthermore, compound **10a** induced complete tumor regression in xenografted or allografted mice, including those receiving K562, Ku812 human CML cells, or Ba/F3 cells harboring Bcr-Abl ^{WT} or a panel of resistance-related mutants. Compound **10a** also extended survival in an allograft mice model utilizing Ba/F3-Bcr-Abl ^{T315I} cells.

MOLECULAR DESIGN AND COMPUTATIONAL STUDIES

Compound **8** is a recently disclosed pan Bcr-Abl inhibitor that demonstrated promising efficacy in imatinib-resistant CML patients in a phase II clinical investigation. [34] X-ray crystallographic analyses revealed that compound **8** bound the DFG-out modes of Bcr-Abl ^{WT} and the Bcr-Abl mutants, and that the imidazo[1,2-*b*]pyridazine core acted as an essential hydrogen bond acceptor for the NH of Met318 in the hinge region of the kinase. The binding mode of compound **8** for Bcr-Abl ^{WT} critically differed from that of compound **1** in that a hydrogen bond was not formed with the hydroxyl group of Thr315. Compound **8** therefore did not suffer the loss of binding affinity for the Bcr-Abl ^{T315I} mutant that was observed for compound **1.** The ethynyl linkage of **8** could provide a favorable van der Waals interaction with the I315 mutated residue. Based on the structural information and interaction mode of **8** with the

kinases, a series of 1*H*-pyrazolo[3,4-*b*]pyridine derivatives was designed and synthesized as novel Bcr-Abl inhibitors. We sought to increase the pan-Bcr-Abl binding affinity relative to **8** by introducing an additional hydrogen bond, as this scaffold was predicted to be capable of acting as both a hydrogen bond donor and a hydrogen bond acceptor for the hinge region of the kinase (Figure **2**). [36]

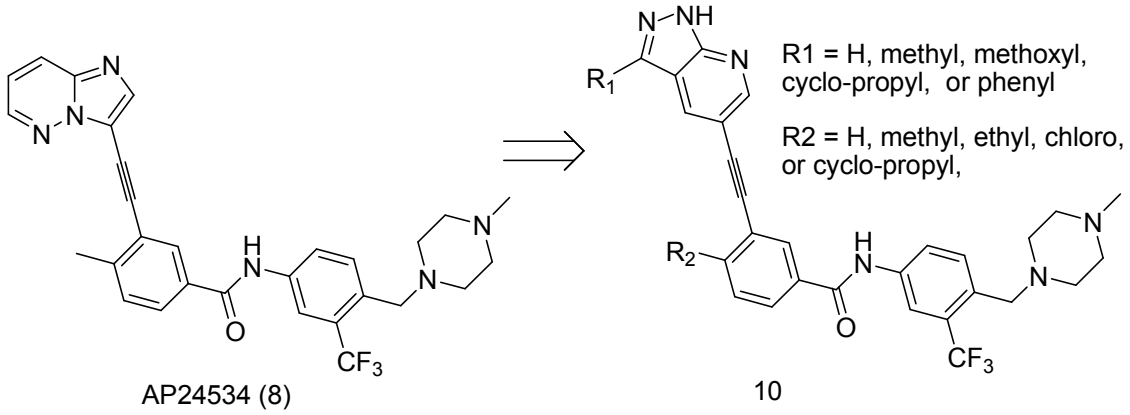

Figure 2. Novel Bcr-Abl inhibitors designed by introducing a 1*H*-pyrazolo[3,4-*b*]pyridine core.

Computational studies were performed to investigate the potential binding mode of the initially designed compound **10a** (R_1 = H; R_2 = Me) with the wild-type and mutant forms of Bcr-Abl. The results suggested that **10a** could tightly bind to the ATP-binding site of non-phosphorylated (DFG-out) Bcr-Abl ^{WT} and different Bcr-Abl mutants, including the clinical-resistance-related Bcr-Abl ^{T315I}, using modes similar to that of **8**. The 1H-pyrazolo[3,4-b] pyridine core occupied the adenine pocket of Bcr-Abl kinase to form a hydrogen bond donor-acceptor network with the backbone of M318 in the hinge region. The amide moiety formed two additional hydrogen bonds with E286 and D381, and the trifluoromethylphenyl group bound deeply into the hydrophobic pocket. The alkyne moiety of **10a** could make favorable van der Waals interactions with the gatekeeper I315 of Bcr-Abl ^{T315I} without causing steric clash. The methylpiperazine group may form hydrogen bond interactions with I360 or H361 (Figure **3A** and **3B**).

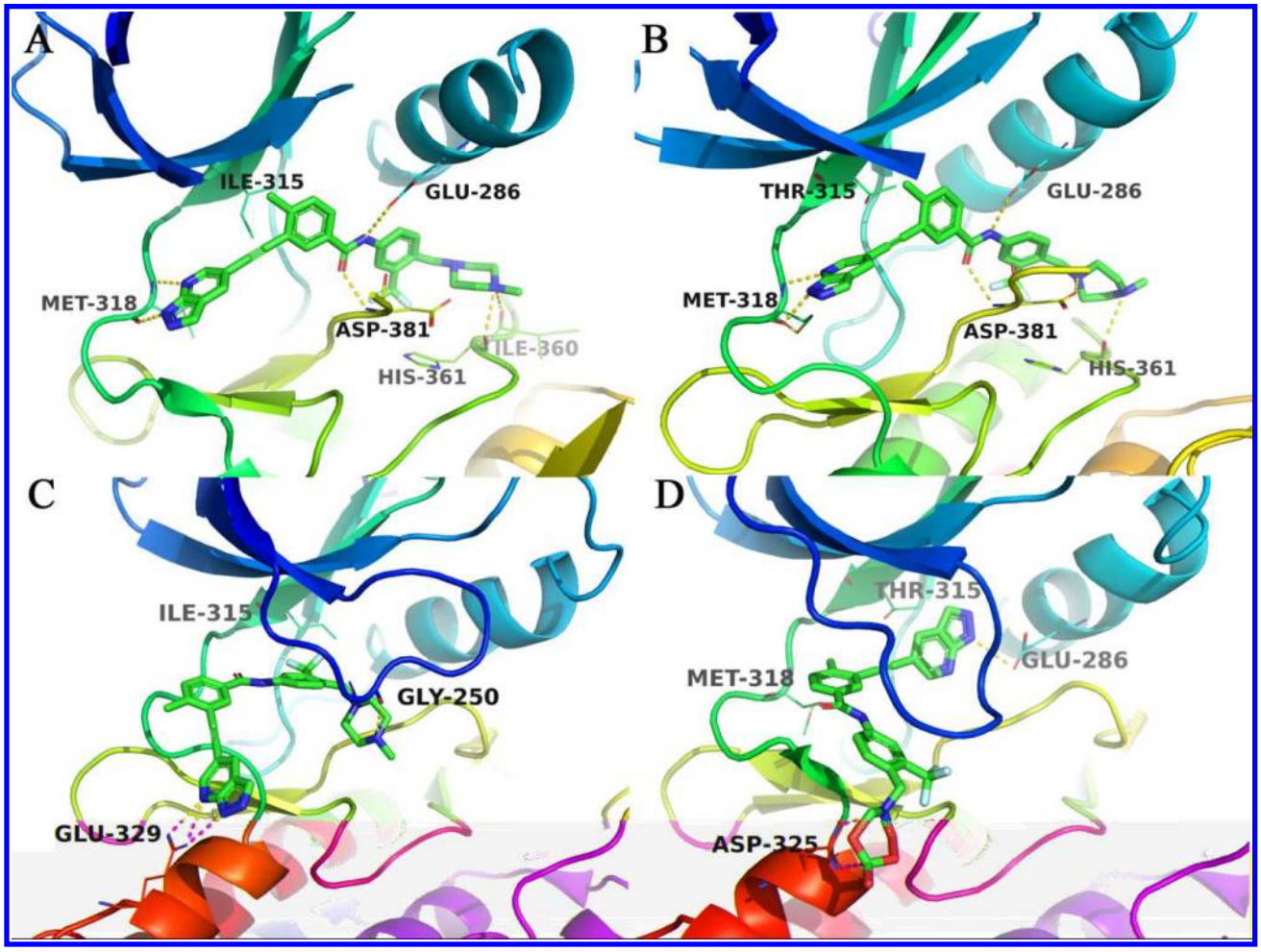

Figure 3. The predicted binding modes of **10a** with the wild-type and mutant forms of Bcr-Abl. Hydrogen bonds to key amino acids are indicated by yellow hatched lines. The following binding modes are shown: A) **10a** with the non-phosphorylated Bcr-Abl ^{T315I} mutant (GScore = -14.82 kcal/mol); B) **10a** with non-phosphorylated native Bcr-Abl (GScore = -13.94 kcal/mol); C) **10a** with the phosphorylated Bcr-Abl ^{T315I} mutant (GScore = -8.63 kcal/mol); and D) **10a** with phosphorylated native Bcr-Abl (GScore = -9.76 kcal/mol). The crystal structures of type I conformations of wild-type and Bcr-Abl ^{T315I} mutant were taken from PDB (ID 3QRI and 3IK3). The PDB codes of the crystal structures of type II conformations of wild-type and Bcr-Abl ^{T315I} mutant were 2GQG and 2V7A, respectitively.

Interestingly, further computational analyses indicated that **10a** could also bind to the ATP-binding site of phosphorylated Bcr-Abl with a DFG-in conformation. Because of the significant differences of activation loop between the DFG-in and DFG-out conformation of Bcr-Abl, the predicted binding mode of **10a** is greatly different from the mode proposed for non-phosphorylated kinases. As shown in Figure

3C and **3D**, a large part of **10a** extended out of the ATP-binding pocket and protruded toward solvent-exposed section of the protein. In the predicted binding pose of **10a** with activated Bcr-Abl ^{T315I}, a hydrogen bond donor-acceptor network could form between the 1H-pyrazolo[3,4-b] pyridine core and the carboxyl group of E329. The methylpiperazine group extended to the pocket form by the P-loop, the DFG motif and the catalytic loop, and may form a hydrogen bond interaction with the backbone of G250. For the DFG-in conformation of wide-type Bcr-Abl (PDB ID 2GQG), Y253 of the P-loop pointed to the activation loop and seemed to engage in a hydrogen bond with the backbone carbonyl of R367, and this motif couldn't be occupied by the ligand. In the docking pose of phosphorylated native Bcr-Abl (Figure 3D), **10a** extended out further toward solvent-exposed protein, and the methylpiperazine group could form hydrogen bond interactions with D325. The 1H-pyrazolo[3,4-b] pyridine moiety pointed to the α C-helix and probably formed a hydrogen bond interaction with E286. The methylphenyl group occupied the ATP-binding site to make favorable hydrophobic interactions with the side chains of F317 and M318. However, the results clearly demonstrated that the predicted GScores of **10a** with DFG-out conformations of Bcr-Abl ^{T315I} mutant and Bcr-Abl ^{WT} (-14.82 kcal/mol and -13.94 kcal/mol, respectively) were significantly lower than that with DFG-in conformations (-8.63 kcal/mol and -9.76 kcal/mol, respectively), suggesting that **10a** prefers to bind with DFG-out conformation of Bcr-Abl. A recent study on DCC2036 (**9**) also implied that **10a** might bind with the phosphorylated Bcr-Abl and the mutants, which exist predominately in the type I conformation, by inducing them to adopt a DFG-out-like conformation. [35a]

CHEMISTRY

The designed inhibitors were readily prepared using palladium-catalyzed Sonogashira coupling reactions as the key steps (Scheme **1** and **2**). [37] Briefly, commercially available or self-prepared methyl 3-iodo-benzoates (**11**) were treated with 4-((4-methylpiperazin-1-yl) methyl)-3-(trifluoromethyl) benzenamine (**12**) under basic conditions to yield the amides (**13**). The intermediates **13** were reacted with ethynyltrimethylsilane under palladium catalysis to afford the Sonogashira coupling products, which were further deprotected to produce the terminal alkynes **14**. The coupling of compounds **14** with

aromatic bromides **18** under Sonogashira conditions, followed by deprotection, afforded the designed inhibitor **10**. Alternately, compound **10b** was obtained by a palladium-catalyzed Sonogashira coupling reaction of **13** with the readily prepared aromatic ethyne **19**. Compounds **18a-18c** and **19** were readily prepared using 5-bromo-1*H*-pyrazolo[3,4-*b*]pyridine (**15**) as the starting material, whereas **20** was synthesized from methyl 5-bromo-2-chloronicotinate (**21**) in three steps. The methanesulfonic acid salt of **10a** (GZD824) was prepared after the free base was reacted with methanesulfonic acid in a quantitative yield. Compounds **24a**, **24b** and **25** were prepared from the key intermediate **14** via Sonogashira coupling with 5-bromo-1*H*-indazole (**26a**), 5-bromo-1-methyl-1*H*-pyrazolo[3,4-*b*]pyridine (**26b**) or 6-bromo-[1,2,4]triazolo[1,5-*a*]pyrimidine (**27**), respectively (Scheme **2**).

Scheme 1. Chemical syntheses of designed inhibitors **10a** – **10i**.

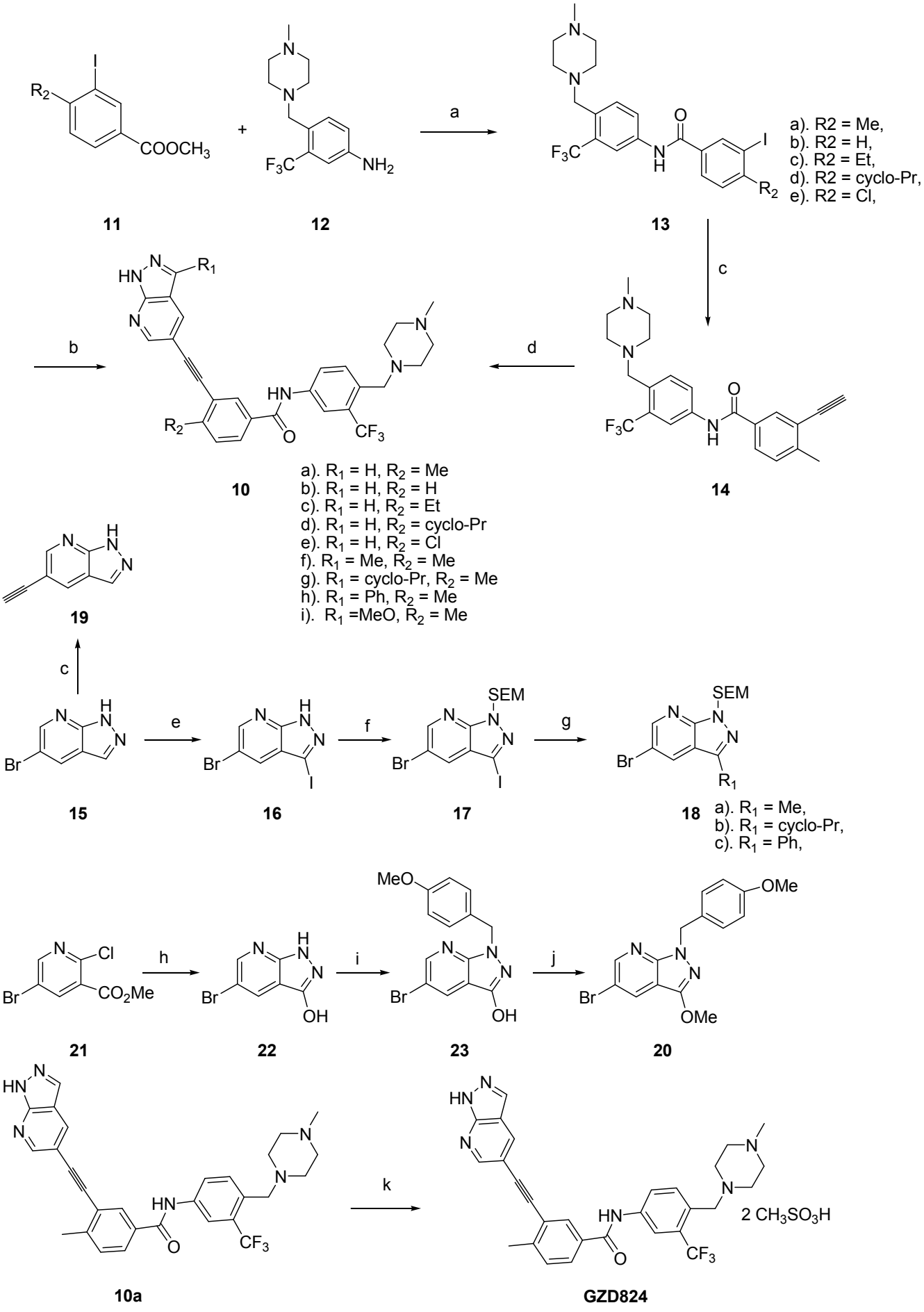
a). R2 = Me,
b). R2 = H,
c). R2 = Et,
d). R2 = cyclo-Pr,
e). R2 = Cl,
11
12
13
14
10
a). R1 = H, R2 = Me
b). R1 = H, R2 = H
c). R1 = H, R2 = Et
d). R1 = H, R2 = cyclo-Pr
e). R1 = H, R2 = Cl
f). R1 = Me, R2 = Me
g). R1 = cyclo-Pr, R2 = Me
h). R1 = Ph, R2 = Me
i). R1 =MeO, R2 = Me
19
15
16
17
18
a). R1 = Me,
b). R1 = cyclo-Pr,
c). R1 = Ph,
21
22
23
20
10a
GZD824
2 CH3SO3H

Reagents and conditions: a) t-BuOK, THF, -20 ^{o}C to r.t., argon, 40-91%; b) $Pd(dppf)_2Cl_2$, CuI, compound **19**, DIPEA, DMF, 80 ^{o}C, 40-75%; c) (i) $Pd(dppf)_2Cl_2$, CuI, ethynyltrimethylsilane, DIPEA, CH_3CN, 60 ^{o}C; (ii) K_2CO_3, MeOH. 79%; d) (i) $Pd(dppf)_2Cl_2$, CuI, compounds **18a-c**, DIPEA, DMF, 80 ^{o}C; (ii) t-Bu_4NF, THF, reflux, 5 hrs. 29-45 %; e) NIS, 1,2-dichloroethane, 66%; f) SEM-Cl, NaH, DMF, 63%; g) $R_1B(OH)_2$, $Pd(dppf)Cl_2$, K_3PO_4, dioxane, 37-57%; h) NH_2NH_2-H_2O, EtOH, 80 ^{o}C, overnight, 93%; i) NaOH, DMSO, p-methoxylbenzyl chloride, rt, 1 hr, 62%; j) NaH, MeI, DMF, rt, overnight, 47%; k) methanesulfonic acid, EtOH, 97%.

Scheme 2. Chemical syntheses of designed inhibitors **24a**, **24b**, and **25**.

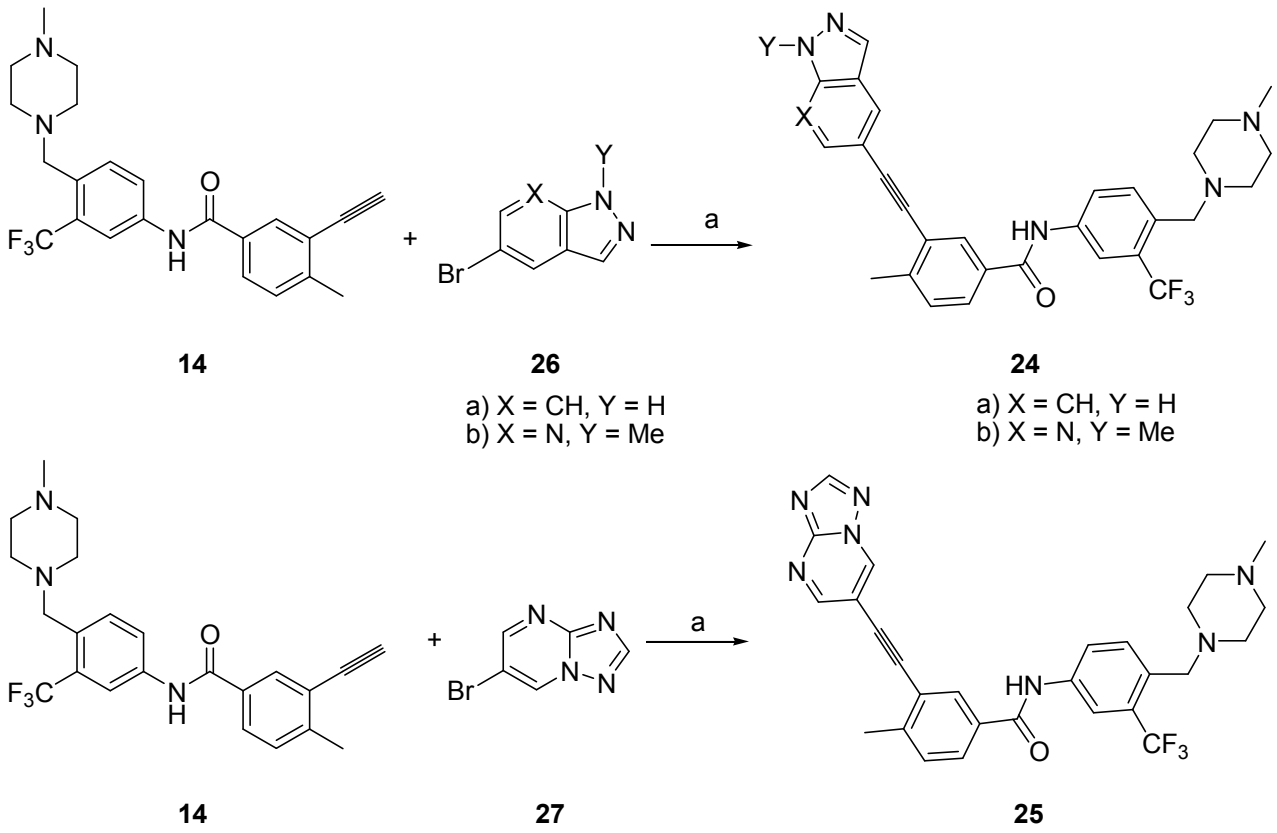

Reagents and conditions: a) $Pd(dppf)_2Cl_2$, CuI, DIPEA, DMF, 80 ^{o}C, 50-55%.

RESULTS AND DISCUSSION

The kinase inhibitory activity of designed compounds **10a** - **10i**, **24** and **25** against different types of Abl kinases were evaluated by using a well-established FRET-based Z'-Lyte assay. [38] Three FDA-approved Bcr-Abl inhibitors [imatinib (**1**), nilotinib (**2**) and dasatinib (**3**)] were used as positive controls to validate the screening conditions. Inhibitor **8** was also included for a direct comparison. As shown in Table **1,** under the experimental conditions, **1** potently inhibited the enzymatic activity of Abl ^{WT} with an IC_{50} value of 98.2 nM, which is highly comparable to the reported data. [35a] However, **1** was

significantly less potent for kinases harboring mutations. Although **2** and **3** were potently inhibited Abl ^{WT} and several of the mutants, they were inactive against the resistance-related T315I mutant. As observed in the reported data, compound **8** suppressed the enzymatic activity of native Abl kinase and all of the 7 resistance-related mutants tested, including the T315I mutation, with low nM IC_{50} values.[34]

Our computational studies suggest that the 1*H*-pyrazolo[3,4-b]pyridine core in **10a** could form a hydrogen bond donor-acceptor network with the hinge region of Bcr-Abl to achieve better protein binding than **8** (Figure **2**). The novel inhibitor **10a** indeed displayed strong inhibition of Abl ^{WT} and a panel of mutants with IC_{50} values that were approximately 2-3 folds lower than the values obtained for compound **8**. For instance, the IC_{50} values of **8** were 1.39, 1.08 and 1.43 nM against Abl ^{T315I}, Abl ^{E255K} and Abl ^{G250E}, respectively, whereas the corresponding values for **10a** were 0.68, 0.27 and 0.71 nM, respectively (Table **1**). To confirm the key contribution of the dual hydrogen bond network formed by the 1*H*-pyrazolo[3,4-b]pyridine core with the hinge region of Bcr-Abl to the activity of **10a**, compounds **23a**, **23b** and **24** were designed and synthesized. Compound **23a** lacks a hydrogen bond acceptor in the hinge-binding region. The IC_{50} values of this compound were 13.9, 82.2, 34.8, 48.6, 29.1, 12.7, 20.1 and 52.6 nM against Abl ^{WT}, Abl ^{T315I}, Abl ^{E255K}, Abl ^{G250E}, Abl ^{Q252H}, Abl ^{H396P}, Abl ^{M351T} and Abl ^{Y253F}, respectively; thus, this compound was 40-120-fold less potent than **10a**. The removal of a hydrogen bond donor in the hinge-binding region (**23b** and **24**) also induced an obvious loss of potency.

A minor structural modification was also introduced to investigate the potential impact of R_1 and R_2 on Abl kinase inhibition (Table **1**). Although many studies have demonstrated that the "flag-methyl" group at the R_2 position is critical for compound **1** and many other Bcr-Abl inhibitors to maintain their kinase inhibition, compound **10b**, in which the methyl group was removed, displayed potency comparable to that of **10a**. However, when the methyl group in the R_2 position was replaced by slightly larger substituents, such as ethyl (**10c**), cyclopropyl (**10d**) or Cl (**10e**), the kinase inhibitory activity was decreased. For instance, the IC_{50} values of compound **10d** against Abl ^{T315I}, Abl ^{E255K} and Abl ^{G250E} were 53.73, 11.38, and 28.71 nM, respectively; thus, this compound was 40-100-fold less potent than **10a**.

The results also clearly revealed that substitution at the R_1 position greatly impacts the inhibitory potency of compounds **10f** – **10i**. Although compound **10f** with a methyl group in the R_1 position displayed a potency similar to that of inhibitor **10a**, compounds **10g** (R_1 = cyclic propyl), **10h** (R_1 = phenyl), and **10i** (R_1 = methoxyl) were obviously less potent than **10a**. For example, the IC_{50} values for **10i** were approximately 25 times higher than those for **10a** against Abl ^{WT} or the Abl ^{T315I} mutant. The detrimental effect of R_1 substitution may be related to increased steric hindrance that makes it unfavorable for the 1*H*-pyrazolo[3,4-b]pyridine core to form hydrogen bonds with the hinge region of Bcr-Abl kinase.

Table 1. Inhibitory activity of the designed compounds against Abl ^{WT} and different mutants. [a]

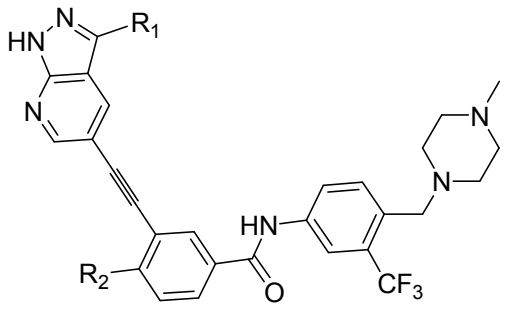

10

cpds			Abl1 inhibition (IC_{50}, nM)							
	R_1	R_2	Native	T315I	E255K	G250E	Q252H	H396P	M351T	Y253F
10a	H	Me	0.34± 0.07	0.68± 0.11	0.27± 0.03	0.71± 0.05	0.15± 0.01	0.35± 0.11	0.29± 0.02	0.35± 0.05
10b	H	H	0.58± 0.10	0.76± 0.17	0.99± 0.11	0.81± 0.09	0.39± 0.10	0.46± 0.03	0.36± 0.01	0.17± 0.01
10c	H	Et	1.92± 0.07	2.36± 0.15	4.93± 0.34	4.08± 1.17	1.14± 0.13	9.39± 0.55	0.94± 0.09	1.28± 0.07
10d	H	Cyclo-Pr	7.1±0.7	53.73 ±1.20	11.38 ±2.37	28.71 ±5.20	3.27± 0.20	2.16± 0.18	2.93± 0.23	4.44± 1.11
10e	H	Cl	0.83± 0.13	1.09± 0.05	2.16± 0.07	3.47± 0.35	0.58± 0.15	0.65± 0.11	0.57± 0.05	0.77± 0.03
10f	Me	Me	0.75± 0.15	0.75± 0.09	1.30± 0.28	1.51± 0.05	0.61± 0.07	0.53± 0.12	0.63± 0.06	0.54± 0.05

10g	Cyclo -Pr	Me	0.84± 0.01	2.07± 0.35	2.90± 0.05	4.08± 0.39	0.92± 0.27	0.43± 0.12	0.93± 0.35	1.15± 0.07
10h	Ph	Me	4.8±1. 05	3.38± 0.09	10.58 ±0.55	9.02± 0.83	3.47± 0.03	3.79± 0.08	2.06± 0.06	2.57± 0.56
10i	MeO	Me	7.9±0. 39	15.81 ±0.58	16.53 ±3.09	36.56 ±1.27	5.02± 2.07	2.72± 0.09	4.28± 0.12	5.15± 0.09
24a			13.9± 0.58	82.2± 0.79	34.8± 5.87	48.6± 7.27	29.1± 0.59	12.7± 0.00	20.1± 1.35	52.6± 2.48
24b			1.49± 0.05	3.20± 0.09	5.40± 0.21	5.04± 0.09	1.08± 0.10	0.71± 0.11	0.76± 0.11	1.06± 0.07
25			3.20± 0.83	6.10± 0.63	9..52± 1.07	18.30 ±5.29	2.03± 0.77	1.38± 0.29	1.33± 0.07	3.26± 0.01
1			98.2± 2.65	5155	485.8 ±55.7	359.9 ±123. 5	115±2 .3	173.9 ±15.8	114.3 ±5.80	749.6 ±66.7
2			43.5± 5.8	702.4 ±37.7	27.8± 5.7	215.3 ±16.8	24.2± 0.9	15.8± 1.8	12.8± 5.7	29.9± 3.2
3			0.26± 0.03	1450	0.21± 0.11	0.25± 0.05	0.24± 0.13	0.30± 0.05	0.22± 0.03	0.17± 0.01
8			0.33± 0.03 (0.37)[b]	1.39± 0.07 (2.0)[b]	1.08± 0.09	1.43± 0.13	0.32± 0.01 (0.44)[b]	0.43± 0.15 (0.34)[b]	0.41± 0.22 (0.30)[b]	0.50± 0.18 (0.30)[b]

[a] The kinase inhibitory activities were determined using a FRET-based Z'-Lyte assay. The data represent the mean values of 3 independent experiments. [b] Reported data. [34]

The direct binding affinity of compound **10a** with the native Abl kinase and the Abl mutants was determined by using a Kinome screening assay based on active-site-dependent competition (conducted by Ambit Bioscience, San Diego, USA). Compound **10a** tightly bound to the ATP-binding sites of the kinases of native Abl and retained the same affinity towards six other frequently detected mutants, including the most refractory gatekeeper mutant T315I as well as those with point mutations in the p-loop (Q252H, E255K), the ATP-binding hinge (F317L/I), the SH2-contact region (M351T) and the activation loop (H396P) (Table **2**). Notably, **10a** displayed similar binding affinities for non-phosphorylated and phosphorylated forms of Abl kinase. For instance, the binding constant values (K_d)

were 0.32 and 0.34 nM for **10a** to bind with nonphosphorylated and phosphorylated Abl, respectively. Compound **10a** also tightly bound with nonphosphorylated and phosphorylated Abl ^{T315I} mutants with K_d values of 0.71 and 3.2 nM, respectively. The selectivity profile of **10a** against a panel of 442 kinases was also investigated at a concentration of 10 nM which was about 33 times of its K_d values on native Abl (Supporting Information). The results clearly revealed that compound **10a** also exhibited strong binding with b-RAF, DDR1, FGFR, Flt3, Kit, PDGFRα, PDGFRβ, RET, Src, Tie1 and Tie2 and several other kinases, indicating that this compound might be used as a lead compound for treatment of many other types of cancer. However, the potential safety issue of **10a** related to its relative kinase selectivity requires further investigation.

Table 2. Binding affinity of **10a** to different mutants of Abl as determined by an active-site-dependent competitive binding assay (Kinomescan Screening). [a]

Abl1	Binding affinity (K_d nM)	
	Non-phosphorylated form	Phosphorylated form
Wild type	0.32	0.34
T315I	0.71	3.20
Q252H	0.46	NA
E255K	NA	0.28
F317I	1.8	NA
H396P	0.18	NA
M351T	NA	0.23

[a] Binding constant values (K_d) were determined from Ambit KINOMEscan ^{TM}. The data represent the mean values of 2 independent experiments.

The Bcr-Abl-inhibitory activity of **10a** was further validated at the cellular level after its antiproliferative activity was evaluated in stably transformed Ba/F3 cells whose growth was driven by native Bcr-Abl or Bcr-Abl mutants, which are mostly responsible for imatinib resistance observed in the

clinic. [39 - 41] The mutants included T315I, L248V, G250E, Q252H, Y253H/F, E255K/V, F317L/V, M351T, E355G, F359V, H396R and F486S, some of which have been frequently reported to be moderately resistant or resistant to compounds **2** or **3**. As shown in Table **3**, **10a** potently inhibited the growth of Ba/F3 cells expressing native Bcr-Abl with an IC_{50} value of 1.0 nM, which was equivalent to the potency of compound **3** (1.9 nM) and much higher than the potency of compounds **1** (460 nM) and **2** (22 nM).

Highly consistent with its potent biochemical kinase inhibition and tight protein binding affinity**, 10a** also strongly inhibited the proliferation of Ba/F3 cells that stably expressed the most refractory Bcr-Abl ^{T315I} mutant, with an IC_{50} value of 7.1 nM. All of the 3 FDA-approved drugs (**1** - **3**) did not inhibit the proliferation of these cells. Furthermore, **10a** displayed a similar potency of inhibition against Ba/F3 cells expressing 14 other resistance-relevant Bcr-Abl mutants. Notably, **10a** was > 50 times less active against parental Ba/F3 cells than Ba/F3 cells expressing Bcr-Abl kinases, which supports its selective inhibition of Bcr-Abl kinase.

Table 3. Inhibition of cellular proliferation as determined using the CCK-8 assay (IC_{50} values, μM) for **10a** and 3 clinically approved Bcr-Abl inhibitors in Ba/F3 cells expressing a panel of Bcr-Abl mutants. [a]

Mutated region	Ba/F3 Cells	Growth inhibition (IC_{50}, μM)			
		1	**2**	**3**	**10a**
	Parental	13.5±2.1	15.1±0.7	2.5±0.3	0.170±0.05
Wild-type	WT	0.5±0.1	0.022±0.005	0.0019±0.0004	0.001±0.0003
	L248V	12.2±0.8	3.0±0.5	0.029±0.011	0.0073±0.0031
	G250E	5.2±1.3	0.15±0.12	0.0051±0.0012	0.006±0.0007
	Q252H	3.6±0.9	0.12±0.05	0.008±0.002	0.006±0.001
P-loop	Y253F	9.2±2.3	1.4±0.7	0.017±0.011	0.011±0.005
	Y253H	12.5±2.5	1.0±0.3	0.0023±0.0012	0.003±0.001
	E255V	>10	1.2±0.1	0.023±0.009	0.0081±0.0012

	E255K	5.6±0.87	0.17±0.07	0.0032±0.0006	0.0035±0.0011
Gate keeper	T315I	12.2±2.1	16.0±1.9	3.6±1.7	0.0071±0.0013
Hinge region	F317L	3.3±0.1	0.16±0.03	0.019±0.013	0.0027±0.0010
	F317V	9.5±3.7	2.9±0.5	0.025±0.006	0.0040±0.0010
SH2-contact region	M351T	0.24±0.06	0.003±0.001	0.0002±0.00003	0.0002±0.00007
Substrate-binding region	E355G	1.6±0.1	0.13±0.03	0.015±0.005	0.0026±0.0007
	F359V	0.59±0.13	0.12±0.07	0.0013±0.0003	0.0023±0.0005
A-loop	H396R	11.1±2.7	21.1±3.9	3.8±2.4	0.0055±0.0010
C-terminal lobe	F486S	1.0±0.3	0.0095±0.0015	0.0009±0.0001	0.0010±0.0003

[a] IC_{50} values are determined by using the cell counting kit (CCK-8) assay. The data represent the mean values of 3 independent experiments.

The antiproliferative activity of **10a** was also examined against a panel of leukemia cells with differing Bcr-Abl status. Taxol was utilized as a positive control to validate the screening conditions. Table **4** shows that **10a** strongly inhibited the growth of leukemia cells positively expressing Bcr-Abl, including K562 and Ku812 human CML cells as well as SUP-B15 human acute lymphocyte leukemia (ALL) cells, with IC_{50} values of 0.21, 0.13 and 2.5 nM, respectively. As a further confirmation of **10a**'s Bcr-Abl-selective effect, **10a** was significantly less potent against the proliferation of MOLT4 and HL-60 leukemia cells, which are negative for Bcr-Abl expression. Not surprisingly, the cytotoxic agent Taxol, which was included in our experiment as a control, inhibited the growth of all tested cells with similar IC_{50} values. K562R is a self-established imatinib-resistant K562 cell line that has been demonstrated to carry a Q252H mutation in Bcr-Abl. **10a** also potently inhibited the proliferation of this cell line with an IC_{50} value of 4.5 nM. Collectively, these results strongly indicate that **10a** selectively inhibits the proliferation of Bcr-Abl -positive tumor cells.

Table 4. Compound **10a** selectively and potently inhibits the proliferation of Bcr-Abl positive leukemia cells.

Cell lines	IC_{50} values (nM, (X±SD)	
	10a	TAXOL
K562	0.2±0.1	5.1±0.5
K562R(Q252H)	4.5±0.7	7.0±0.5
Ku812	0.13±0.02	5.3±3.2
SUP-B15	2.5±1.0	8.0±3.4
U-937	390.2±153.4	2.3±0.2
MOLT4	26.3±10.2	2.7±0.9
HL-60	348.9±158.2	5.8±1.5

[a] IC_{50} values were determined by using the cell counting kit (CCK-8) assay. The data represent the mean values of 3 experiments.

To further validate the cellular kinase inhibitory activity of **10a**, we examined its effects on the activation of Bcr-Abl and its downstream signals in Bcr-Abl-positive K562 CML cells and stably transformed Ba/F3 cells expressing native Bcr-Abl or Bcr-Abl ^{T315I} (Figure **4**) by Western blot analyses. **10a** efficiently suppressed the activation of Bcr-Abl as well as downstream Crkl and STAT5 in a concentration-dependent manner in K562 CML cells. Similar inhibition was also observed in Ba/F3 cells expressing native Bcr-Abl or Bcr-Abl ^{T315I}. Not surprisingly, none of the 3 FDA-approved drugs demonstrated an obvious suppression of Bcr-Abl ^{T315I} activation.

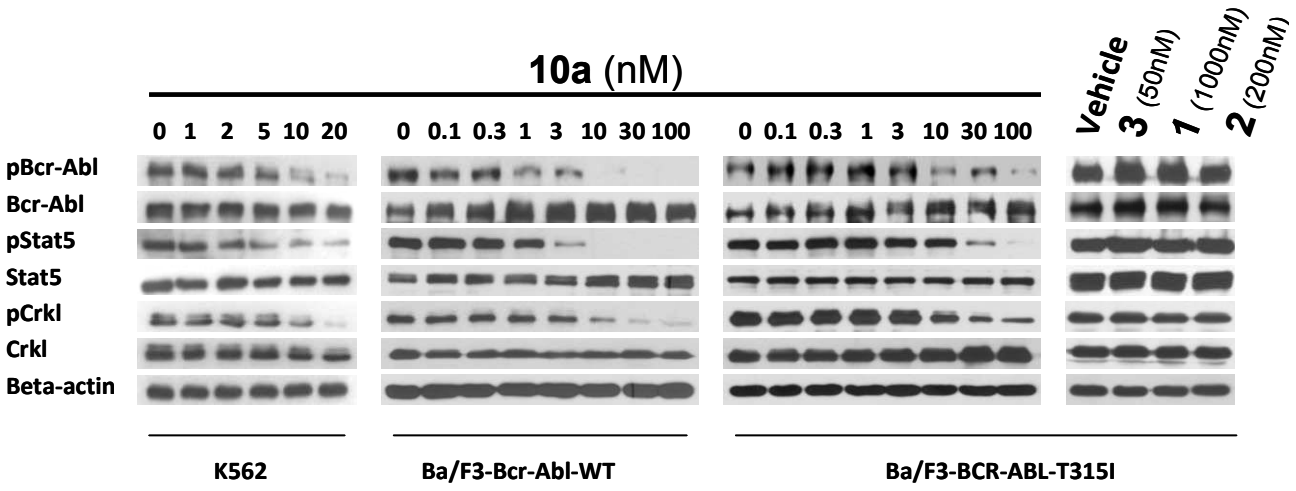

Figure 4. Compound **10a** inhibits Bcr-Abl signaling in K562 and Ba/F3 stable cell lines expressing native Bcr-Abl or Bcr-Abl ^{T315I}. Cells were treated with **10a** at the indicated concentrations for 4.0 hours and whole cell lysates were then subjected to western blot analyses. The results represent 3 independent experiments (**1**, imatinib; **2**, nilotinib; **3**, dasatinib).

Given its highly promising *in vitro* kinase inhibition and antiproliferative activity, we further investigated the preliminary ADME (absorption, distribution, metabolism and excretion) profiles of compound **10a**, and it displayed good metabolic stability as determined by an *in vitro* rat microsomal stability assay. [42] The half-life ($T_{1/2}$) of **10a** was approximately 56 minutes, and its intrinsic clearance (CL_{int}) was approximately 36.4 μL/min/mg. Furthermore, a cytochrome P450 inhibitory assay [43] revealed that **10a** did not obviously inhibit CYP1A2, CYP2D6, CYP3A4 and CYP2E1 at 30 μM. However, **10a** potently inhibited CYP2C9 and CYP2C19 with IC_{50} values of 0.11 and 0.99 μM respectively, which indicates that it may be subject to potential drug-drug interactions with other medicinal products, which are metabolized primarily by CYP2C9 and CYP2C19. The transcellular diffusional permeability and transport directionality of **10a** were also determined by using the well-established model of Caco-2 cells, which express efflux transporters, such as P-glycoprotein. [44] The apical-to-basolateral and basolateral-to-apical permeabilities of **10a** were 3.2 and 2.8 nm/s, respectively.

Thus, **10a** exhibits good bidirectional permeability in Caco-2 cells. The permeability directional ratio (efflux ratio) for **10a** was 0.90, and **10a** thus did not appear to be a substrate for P-glycoprotein efflux transporters. [45]

An *in vivo* pharmacokinetic (PK) evaluation of the bismesylate salt of **10a** (GZD824) was also conducted in rats. Plasma levels of **10a** were monitored after a single oral dose of 25 mg/kg. The C_{max} (390.5 μg/L = 733 nM) occurred at 4.0 hours post-dose and was > 500 times higher than the *in vitro* IC_{50} values in Bcr-Abl-positive CML cells and Ba/F3 cells expressing different Bcr-Abl mutants, including Bcr-Abl ^{T315I}. The half-life of **10a** was 10.6 hours. The plasma levels of **10a** were approximately 270 and 169 nM at 12 and 24 hours post-dose, respectively (Table **4**). Good oral bioavailability (48.7%) and an ideal half-life suggest that **10a** may have good *in vivo* efficacy when orally administrated.

Table 4. The bismesylate salt of compound **10a** (GZD824) displays a good pharmacokinetic profile in rats.

Pharmacokinetic parameters for **10a**									
Routes	C_{max} (μg/L)	T_{max} (hr)	AUC_{0-t} (μg/L* h)	$AUC_{0-\infty}$ (μg/L*h)	$T_{1/2}$ (hr)	MRT (hr)	CL (L/h/kg)	V_{ss} (L/kg)	F (%)
I.V. (5mg/kg)	1375.6	0.067	2737.3	2922.4	5.6	6.7	1.7	13.7	
Oral (25mg/kg)	390.5	4.0	6699.0	7108.2	10.6	17.9	3.6	53.2	48.7%

The human ether-a-go-go-related gene (hERG) encodes an inward rectifying voltage-gated potassium channel in the heart (IKr) that is involved in cardiac repolarization. Inhibition of the hERG can cause QTc interval prolongation, which is associated with potential lethal arrhythmias known as torsadesde pointes. [48] The potential cardiotoxicity of **10a** was also initially examined by using a nonradioactive rubidium (Rb^+) efflux assay. [49] Compound **10a** did not show appreciable activity against the hERG

potassium channel at concentrations of ≤ 30 μM, which suggests that it may have little or no cardiotoxic effects (Supporting Information).

The i*n vivo* anti-tumor effect of **10a** was first evaluated in subcutaneous K562 and Ku812 xenograft models of human CML. The clinical drug **1** was used as a positive control to validate the animal models. As shown in Figure **5**, **10a** dose-dependently inhibited the growth of the K562 tumor xenograft when administrated once daily for 14 consecutive days *via* oral gavage. A significant reduction in tumor size was observed after only 2 days of treatment at doses of 2, 5 and 10 mg/kg/day (p = 0.03, 0.002 and 0.002, respectively). Compound **10a** almost completely eradicated the tumor at doses of 5 and 10 mg/kg/day after only 6 days of treatment, whereas the reference drug **1** only induced tumor stasis at a dose of 50 mg/kg/day. Even at a dose as low as 1 mg/kg/day, **10a** still significantly suppressed tumor growth (68.3% inhibition after 14 days of dosing, $p < 0.01$). Notably, after the cessation of treatment (14 days of dosing), there was no sign of tumor recurrence in the following 20 days for the groups that received 5 and 10 mg/kg/day, and recurrence in the 2 mg/kg/day group was also found to a minor extent (data not shown). All doses of **10a** were well tolerated, with no mortality or significant body loss (< 5% relative to the vehicle-matched controls) observed during treatment. Similar results were also obtained in the Ku812 xenograft model, where even 1.0 mg/kg/day of **10a** induced complete tumor regression after a 14-day treatment period (Supporting Information).

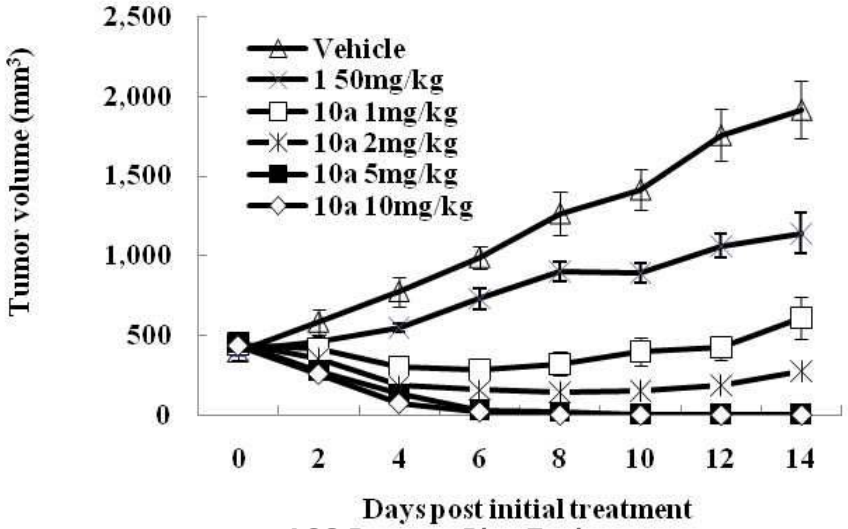

Figure 5. Compound **10a** potently suppresses tumor growth in mice bearing xenografted K562 cells as a model of human CML. Mice bearing K562 xenografts were dosed orally once a day with the indicated compounds at the indicated dosages for 14 consecutive days (n=10 per group, error bars represent the standard error). The data are representative of 2 independent experiments.

The anti-tumor activity of **10a** was also evaluated in allograft models using Ba/F3 cells expressing Bcr-Abl ^{WT}, Bcr-Abl ^{T315I}, Bcr-Abl ^{E255K}, Bcr-Abl ^{G250E} and Bcr-Abl ^{F317L}. As described above, Bcr-Abl ^{T315I} is the most refractory mutant, whereas the p-loop mutants Bcr-Abl ^{E255K} and Bcr-Abl ^{G250E} and the hinge region mutant Bcr-Abl ^{F317L} are frequently detected mutants that drive clinical resistance to many Bcr-Abl inhibitors. For instance, the Bcr-Abl ^{E255K} mutant has been reported to be insensitive to the three classical inhibitors (**1**, **2** and **3**) and the two most recently reported Bcr-Abl inhibitors, **8** and **9**, whereas Bcr-Abl ^{F317L} was also relatively insensitive to **1**, **3** and **9**. The P-loop mutants were also reported to be associated with poor prognoses in the clinic. [46, 47]

Following an experimental design similar to that of the K562 and Ku812 xenograft studies, animals were administrated a range of doses of **10a** *via* oral gavage once daily for 14 days. Compound **1** was again used as a reference compound and administered orally at doses of 50 or 100 mg/kg/day for 14 days. As shown in Figure **6A**, **10a** dose-dependently inhibited tumor growth in the allograft model using Ba/F3 cells expressing Bcr-Abl ^{WT}. A dose of 1.0 mg/kg/day of **10a** exhibited *in vivo* efficacy comparable to that of 50 mg/kg of the reference drug **1**. When the mice received a dose of 5.0 mg/kg/day, **10a** induced complete tumor regression. Additionally, **10a** displayed promising efficacy in the allograft model bearing Bcr-Abl ^{T315I}-driven tumors (Figure **6B**). Although **10a** did not show obvious inhibition of tumor growth at doses of 5 or 10 mg/kg/day in the Bcr-Abl ^{T315I} model, it induced almost complete tumor regression at a dose of 20 mg/kg/day after a 14-day consecutive treatment. In

contrast, 100 mg/kg/day of **1** completely failed to exhibit any inhibition of tumor growth in the Bcr-Abl ^{T315I} model. Moreover, **10a** also significantly reduced the tumor burden by alleviating hepatosplenomegaly, which appears at late stages of this leukemia-like model and is induced by the Bcr-Abl ^{T315I}-driven cells (data not shown). Similar efficacy of **10a** was also observed in the Bcr-Abl ^{G250E} and Bcr-Abl ^{E255K} p-loop mutants as well as Bcr-Abl ^{F317L} hinge-region-mutant-driven tumor allografts (Supporting Information).

The antitumor efficacy of **10a** was further evaluated in a mouse allograft leukemia model, in which Ba/F3 cells expressing Bcr-Abl ^{T315I} were further stably transfected with a luciferase-expressing vector to facilitate non-invasive bioluminescent monitoring of tumor cell proliferation *in vivo*. Ba/F3 cells co-expressing Bcr-Abl ^{T315I} and luciferase were designated as Ba/F3/T315I-Luc cells and injected intravenously into immuno-deficient mice. These cells proliferated in the blood, spleen and bone marrow, eventually leading to the morbidity and death of the recipients. The *in vivo* anti-tumor efficacy of **10a** was therefore evaluated in this model through the measurement of *in vivo* luminescence signals and survival in the recipient mice. Generally, at 7-10 days after inoculation of the Ba/F3-T315-Luc cells, the *in vivo* luminescence signal became detectable in the vehicle-treated control group, which indicates the success of the engraftment. Treatment with the test compounds was then initiated through oral gavage once daily for 10 consecutive days.

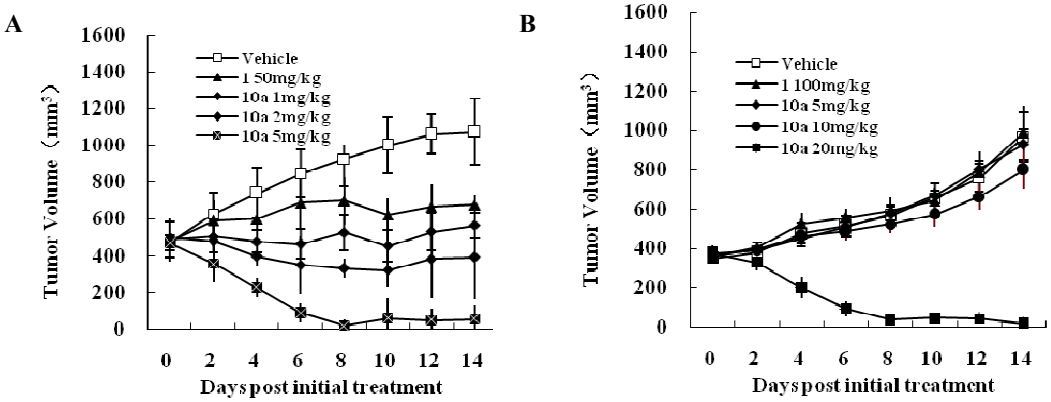

Figure 6. Compound **10a** suppresses tumor growth in mice bearing allografted Ba/F3 cells expressing Bcr-Abl ^{WT} (**A**) and Bcr-Abl ^{T315I} (**B**). Mice bearing allografted Ba/F3 cells expressing the indicated Bcr-Abl mutants were orally dosed with **10a** and **1** at the indicated doses. The tumor sizes were monitored over time (n=10 for each group; error bars represent the SE). The data are representative of 2 or 3 independent experiments.

As shown in Figure 7**A**, luminescence signals representing the populations of Ba/F3-T315I-Luc cells *in vivo* were detected at days 0 and 7 after initiation of treatment. At day 0, it was clear that the average population size of Ba/F3-T315I-Luc cells was almost identical among different groups before the treatment was initiated. At day 7, in the vehicle-only group, luminescence signals were observed throughout the entire bodies of the mice, which suggested that the leukemia-like Ba/F3-T315I-luc cells has disseminated *in vivo*. After treatment with **10a** at 5, 10 or 20 mg/kg/day, the luminescence signals were obviously decreased when compared with the untreated vehicle-only group. Notably, treatment with 20 mg/kg/day of **10a** nearly eliminated the luminescence signals, which indicates complete suppression of the proliferation of the Ba/F3-T315I-Luc cells. Quantification of the luminescence signal clearly revealed that **10a** potently and dose-dependently decreased the signal intensity (Figure **7B**). Although compound **10a** demonstrated significant efficacy in this Bcr-Abl ^{T315I} leukemia model, reference drug **1** was totally inactive at a dose of 100 mg/kg/day. Highly consistent with its strong inhibition of the proliferation of the BaF3/T315I-luc cells, treatment with **10a** significantly prolonged the survival of the mice in a dose-dependent manner in this allograft model, whereas 100 mg/kg of **1** did not show any survival benefit (Figure **7C**). Indeed, following treatment with **10a** for 10 days at doses of 5, 10 and 20 mg/kg/day, the median survival of the mice was significantly increased to 23.7, 24.6 and 31.9 days, respectively, as compared with 18.9 days for the vehicle-treated group. Additionally, hepatosplenomegaly was commonly observed in vehicle-treated mice in the late stages of the survival experiment but was barely detected in the **10a**-treated mice, which indicates that **10a** could efficiently alleviate the tumor burden in late stage leukemia (data not shown).

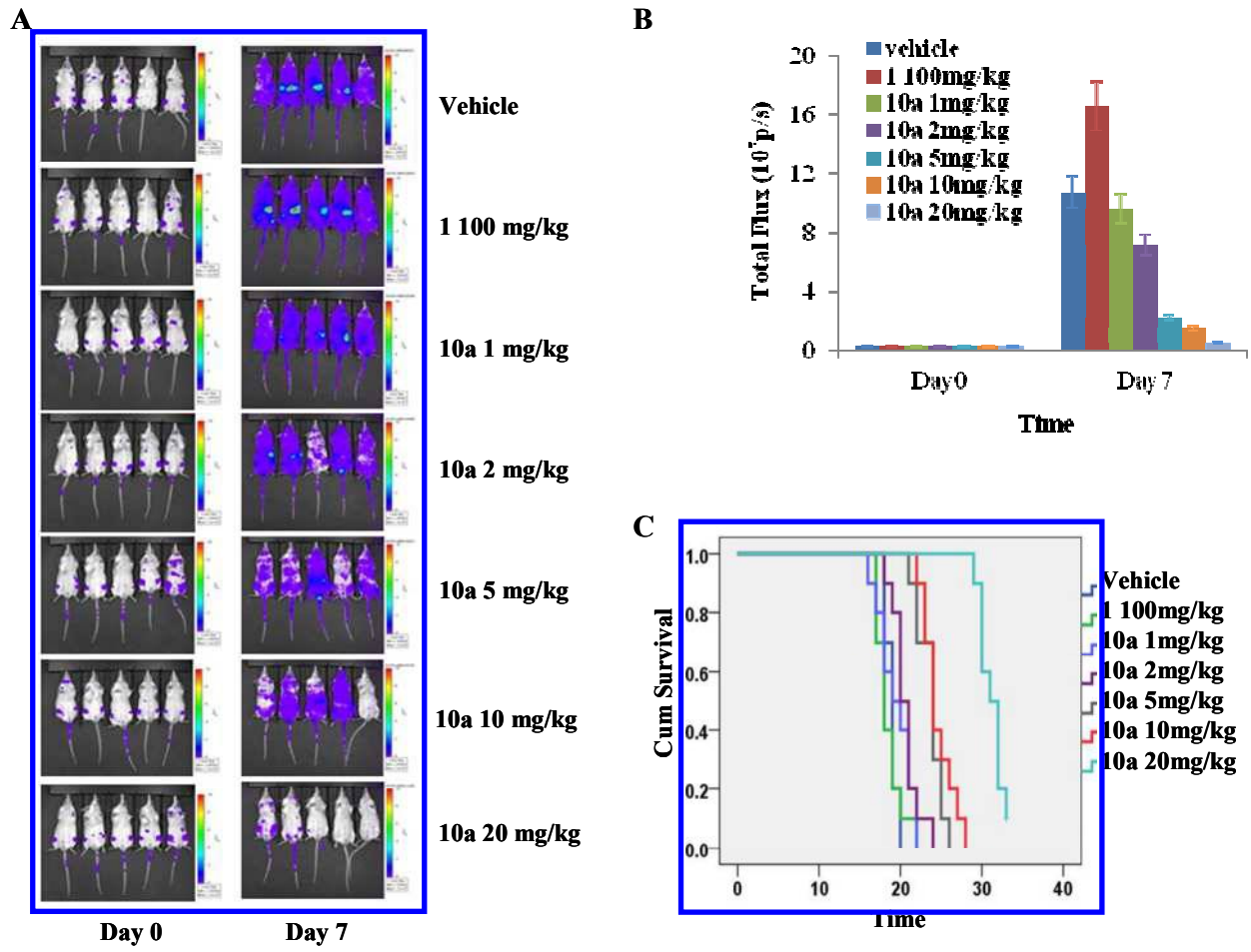

Figure 7. Compound **10a** efficiently prolongs animal survival in an allograft leukemia tumor model using Ba/F3 cells co-expressing Bcr-Abl ^{T315I} and luciferase. A) Compound **10a** suppresses the proliferation of leukemia-like Ba/F3 cells co-expressing Bcr-Abl ^{T315I} and luciferase; B) Quantification of the images in B; C) Compound **10a** prolongs the survival of leukemic mice.

In summary, we have successfully designed and synthesized a series of novel inhibitors that display significant inhibition against a broad spectrum of Bcr-Abl mutants, including those carrying the gatekeeper T315I and the p-loop mutations, which are associated with poor prognosis in CML. One of the most promising compounds, **10a**, tightly binds the phosphorylated and non-phosphorylated forms of Bcr-Abl kinase and inhibits the proliferation of Bcr-Abl-positive human CML cells. Furthermore, compound **10a** potently inhibits the proliferation of a panel of murine BaF3 cells ectopically expressing Bcr-Abl ^{WT} and a broad spectrum of other Bcr-Abl mutants that contribute to clinical TKI resistance,

including the most refractory gatekeeper mutant, Bcr-Abl ^{T315I}. *In vivo* efficacy studies in mouse xenograft or allograft models of human leukemia demonstrated that **10a** successfully suppressed the growth of tumors driven by native Bcr-Abl, Bcr-Abl ^{T315I}, Bcr-Abl ^{G250E,} Bcr-Abl ^{Q252H,} Bcr-Abl ^{E255K} and Bcr-Abl ^{F317L}. Compound **10a** also provided a significant survival benefit leukemia model mice allografted with luciferase-expressing Ba/F3 cells driven by the mutant Bcr-Abl ^{T315I} kinase. The potential for compound **10a** to overcome all of the Bcr-Abl mutations that result in clinically acquired resistance to imatinib indicates that this novel Bcr-Abl inhibitor is a promising lead candidate for further development.

EXPERIMENTAL

Chemistry. Reagents and solvents were obtained from commercial suppliers and used without further purification. Flash chromatography was performed using silica gel (300-400 mesh). All reactions were monitored by TLC, silica gel plates with fluorescence F_{254} were used and visualized with UV light. ^{1}H and ^{13}C NMR spectra were recorded on a Bruker AV-400 spectrometer at 400 MHz and Bruker AV-500 spectrometer at 125 MHz, respectively. Coupling constants (*J*) are expressed in hertz (Hz). Chemical shifts (δ) of NMR are reported in parts per million (ppm) units relative to internal control (TMS). The low or high resolution of ESI-MS was recorded on an Agilent 1200 HPLC-MSD mass spectrometer or Applied Biosystems Q-STAR Elite ESI-LC-MS/MS mass spectrometer, respectively. The purity of compounds was determined to be over 95% (>95%) by reverse-phase high performance liquid chromatography (HPLC) analysis. HPLC instrument: DIONEX SUMMIT HPLC (Column: Diamonsil C18, 5.0 μm, 4.6 x 250 mm(Dikma Technologies); Detector: PDA-100 Photodiode Array; Injector: ASI-100 Autoinjector; Pump: p-680A.). Elution: MeOH in water; Flow rate: 1.0 mL/min.

3-Iodo-4-methyl-N-(4-((4-methylpiperazin-1-yl)methyl)-3-(trifluoromethyl)phenyl)benzamide (**13a**). A solution of **11a** (8.6 g, 31.16 mmol) and 4-((4-methylpiperazin-1-yl)methyl)-3-(trifluoromethyl)aniline (**12**) (8.48 g, 31.16 mmol) in anhydrous THF (150.0 mL) was added potassium tert-butoxide (20.9 g, 186.96 mmol) in anhydrous THF (150.0 mL) at - 20 ^{o}C for 1.0 hr. Then the

reaction mixture was slowly warmed to room temperature and stirred for another 2.0 hrs. After the reaction was finished by TLC, the mixture was poured into 1.0 L water with stirring and then left to stand overnight. The precipitated brown solid was filtered and dried under reduced pressure to afford the desired product. (14.7 g, yield: 91.4%) ^{1}H NMR (400 MHz, $CDCl_3$), δ 8.28 (d, *J* = 1.8 Hz, 1 H), 7.91 (s, 1 H), 7.86 (dd, *J* = 1.9, 8.4 Hz, 1 H), 7.83 (s, 1 H), 7.78 (d, *J* = 8.4 Hz, 1 H), 7.74 (dd, *J* = 1.8, 8.0 Hz, 1 H), 7.33 (d, *J* = 8.0 Hz, 1 H), 3.63 (s, 2 H), 2.50-2.46 (m, 11 H), 2.29 (s, 3 H).

3-ethynyl-4-methyl-N-(4-((4-methylpiperazin-1-yl)methyl)-3-(trifluoromethyl)phenyl)benzamide (**14**). A mixture of **13a** (13.7 g, 26.5 mmol), Cu (I) iodide (0.05 g, 0.26 mmol), $Pd(PPh_3)_2Cl_2$ (0.2 g, 0.26 mmol) were added to a 250 mL round-bottom flask. The flask was evacuated and backfilled with argon (3 cycles). Acetonitrile (100.0 mL), DIPEA (18.1 mL, 106 mmol) and trimethylsilylacetylene (7.48 mL, 53.0 mmol) were added by syringe at room temperature. After stirring at 60 ^{o}C overnight, the reaction mixture was filtered and concentrated. The residue was dissolved in methanol (50.0 mL) with addition of K_2CO_3 (7.31 g, 53 mmol). The reaction mixture was stirred at room temperature for 10~15 minutes, and then filtered and concentrated for further purification through flash column chromatography on silica gel to afford the desired product as pale solid. (8.7 g, yield: 79%) ^{1}H NMR (400 MHz, *d*-DMSO), δ 10.49 (s, 1 H), 8.19 (d, *J* = 2.0 Hz, 1 H), 8.08 (d, *J* = 1.6 Hz, 1 H), 8.03 (dd, *J* = 1.6, 8.4 Hz, 1 H), 7.90 (dd, *J* = 8.0 Hz, 1.6 Hz, 1 H), 7.70 (d, *J* = 8.4 Hz, 1 H), 7.47 (d, *J* = 8.0 Hz, 1 H), 4.51 (s, 1 H), 3.56 (s, 2 H), 2.46 (s, 3 H), 2.33 (br, 8 H), 2.15 (s, 3 H).

3-((1H-Pyrazolo[3,4-b]pyridin-5-yl)ethynyl)-4-methyl-N-(4-((4-methylpiperazin-1-yl)methyl)-3-(trifluoromethyl)phenyl)benzamide (**10a**). A mixture of **13a** (2.60 g, 5.0 mol), **19** (0.72 g, 5.0 mmol), Cu (I) iodide (0.5 g, 0.5 mmol), $Pd(PPh_3)_2Cl_2$ (1.8 g, 0.5 mmol) were added to a sealed tube. The tube was evacuated and backfilled with argon (3 cycles). Acetonitrile (50.0 mL), Et_3N (21.0 mL, 0.1 mol) were added by syringe at room temperature. After stirring at 100 ^{o}C for about 20 hrs, the reaction mixture was filtered and concentrated. The residue purified by flash column chromatography on silica gel to afford the desired product as yellow solid. Yield: 76%. ^{1}H NMR (400 MHz, *d*-DMSO), δ 13.94 (s,

1 H), 10.53 (s, 1 H), 8.74 (d, *J* = 2.0 Hz, 1 H), 8.53 (d, *J* = 2.0 Hz, 1 H), 8.22-8.19 (m, 3 H), 8.07 (dd, *J* = 1.6, 8.4 Hz, 1 H), 7.92 (dd, *J* = 2.0, 8.0 Hz, 1H), 7.71 (d, *J* = 8.4 Hz, 1 H), 7.53 (d, *J* = 8.0 Hz, 1 H), 3.56 (s, 2 H), 2.59 (s, 3 H), 2.39 (br, 4 H), 2.33 (br, 4 H), 2.16 (s, 3 H); ^{13}C NMR (125 MHz, *d*-DMSO), δ 165.11, 151.44, 151.01, 144.12, 138.59, 134.12, 133.42, 132.61, 132.51, 131.65, 130.95, 130.36, 128.56, 127.82 (d, *J* = 30.0 Hz), 124.76 (d, *J* = 272.5 Hz), 123.91, 122.60, 117.68, 114.44, 112.21, 92.33, 88.71, 57.88, 55.14, 53.11, 46.13, 20.85; MS (EI): 533 $[M+H]^+$; Purity: 99.77% (t_R 11.33 min).

3-((1H-Pyrazolo[3,4-b]pyridin-5-yl)ethynyl)-N-(4-((4-methylpiperazin-1-yl)methyl)-3-(trifluoromethyl)phenyl)benzamide (**10b**). This compound was synthesized by reacting **13b** with **19** under similar procedure to that of **10a.** Yield: 51%. ^{1}HNMR (400 MHz, *d*-DMSO), δ 13.94 (s, 1 H), 10.62 (s, 1 H), 8.73 (d, *J* = 2.0 Hz, 1 H), 8.52 (d, *J* = 1.6 Hz, 1 H), 8.23-8.21 (m, 3H), 8.07 (d, *J* = 8.4 Hz, 1 H), 8.01 (d, *J* = 7.6 Hz, 1 H), 7.82 (d, *J* = 7.6 Hz, 1 H), 7.72 (d, *J* = 8.4 Hz, 1 H), 7.63 (t, *J* = 7.6 Hz, 1 H), 3.57 (s, 2 H), 2.39 (br, 4 H), 2.33 (br, 4 H), 2.15 (s, 3 H); ^{13}C NMR (125 MHz, *d*-DMSO), δ 165.25, 151.52, 151.00, 138.51, 135.39, 134.84, 134.14, 133.54, 132.65, 131.68, 130.71, 129.58, 128.62, 127.84, 124.74, 123.94, 122.82, 117.70, 114.41, 111.99, 89.83, 88.55, 57.87, 55.14, 53.12, 46.13; MS (EI): 519 $[M+H]^+$; Purity: 99.71% (t_R 9.73 min).

3-((1H-Pyrazolo[3,4-b]pyridin-5-yl)ethynyl)-4-ethyl-N-(4-((4-methylpiperazin-1-yl)methyl)-3-(trifluoromethyl)phenyl)benzamide (**10c**). This compound was synthesized by reacting **13c** with **19** under similar procedure to that of **10a**. Yield: 40.7%. ^{1}H NMR (400 MHz, d-DMSO), δ 13.95 (s, 1 H), 10.56 (s, 1 H), 8.72 (d, *J* = 2.0 Hz, 1 H), 8.51 (d, *J* = 2.0 Hz, 1 H), 8.22 (s, 2 H), 8.19 (d, *J* = 1.6 Hz, 1 H), 8.07 (dd, *J* = 1.6, 8.4 Hz, 1 H), 7.96 (dd, *J* = 2.0, 8.4 Hz, 1 H), 7.70 (d, *J* = 8.4 Hz, 1 H), 7.53 (d, *J* = 8.0 Hz, 1 H), 3.57 (s, 2 H), 2.95 (q, *J* = 7.6 Hz, 2 H), 2.40 (br, 8 H), 2.20 (s, 3 H), 1.30 (t, *J* = 7.6 Hz, 3 H); ^{13}C NMR (125 MHz, d-DMSO), δ 164.71, 150.90, 150.55, 149.64, 138.18, 133.67, 132.93, 132.27, 131.95, 131.20, 130.83, 18.48, 128.38, 127.38, 124.30, 123.44, 121.45, 117.22, 113.99, 111.76, 91.35, 87.98, 57.35, 55.54, 52.39, 45.57, 45.38, 27.13, 14.49; MS (EI): 547 $[M+H]^+$; Purity: 96.31% (t_R 13.20 min).

3-((1H-Pyrazolo[3,4-b]pyridin-5-yl)ethynyl)-4-cyclopropyl-N-(4-((4-methylpiperazin-1-yl)methyl)-3-(trifluoromethyl)phenyl)benzamide (**10d**). This compound was synthesized by reacting **13d** with **19** under similar procedure to that of **10a**. Yield: 55%. 1H NMR (400 MHz, d-DMSO), δ 13.45 (s, 1 H), 10.54 (s, 1 H), 8.68 (d, *J* = 2.0 Hz, 1 H), 8.54 (d, *J* = 2.0 Hz, 1 H), 8.21 (d, *J* = 2.0 Hz, 1 H), 8.19 (d, *J* = 1.6 Hz, 1 H), 8.07 (d, *J* = 8.4 Hz, 1 H), 7.92 (dd, *J* = 1.6, 8.0 Hz, 1 H), 7.70 (d, *J* = 8.4 Hz, 1 H), 7.52 (d, *J* = 8.0 Hz, 1 H), 3.56 (s, 2 H), 2.59 (s, 3 H), 2.40-2.34 (m, 9 H), 2.15 (s, 3 H), 1.03-1.00 (m, 4 H); ^{13}C NMR (125 MHz, d-DMSO), δ 164.59, 151.00, 150.53, 149.49, 138.15, 133.62, 132.94, 131.97, 131.34, 131.16, 130.56, 128.43, 127.37, 124.29, 123.42, 123.33, 121.92, 117.20, 113.97, 111.84, 91.39, 88.40, 79.17, 78.91, 78.64, 57.39, 55.98, 54.64, 52.57, 45.58, 18.48, 13.86, 10.24; MS (EI): 559 $[M+H]^+$. Purity: 98.36% (t_R 13.24 min).

3-((1H-pyrazolo[3,4-b]pyridin-5-yl)ethynyl)-4-chloro-N-(4-((4-methylpiperazin-1-yl)methyl)-3-(trifluoromethyl)phenyl)benzamide (**10e**). This compound was synthesized by reacting **13e** with **19**under similar procedure to that of **10a**. Yield: 45%. ^{1}H NMR (400 MHz, d-DMSO), δ 13.95 (s, 1H), 10.64 (s, 1 H), 8.73 (s, 1 H), 8.54 (s, 1 H), 8.32 (s, 1 H), 8.23 (s, 1 H), 8.19 (s, 1 H), 8.04 (s, 1 H), 8.01 (s, 1 H), 7.80 (s, 1 H), 7.71 (s, 1 H), 3.55 (s, 2 H), 2.37 (br, 8 H), 2.15 (s, 3 H). ^{13}C NMR (125 MHz, d-DMSO), δ 163.84, 150.98, 150.69, 137.91, 137.84, 133.85, 133.41, 132.35, 132.17, 131.24, 129.69, 129.56, 127.42, 124.28, 123.53, 122.02, 117.27, 114.00, 111.11, 93.16, 86.27, 57.42, 54.69, 52.66, 45.67. MS (EI): 553 $[M+H]^+$. Purity: 97.85% (t_R 13.19 min).

3-((3-Cyclopropyl-1H-pyrazolo[3,4-b]pyridin-5-yl)ethynyl)-4-methyl-N-(4-((4-methylpiperazin-1-yl)methyl)-3-(trifluoromethyl)phenyl)benzamide (**10g**)**.** A mixture of **14** (0.35g, 0.84 mmol), **18b** (0.31 g, 0.84 mmol), Cu (I) iodide (1.6 mg, 0.0084 mmol), $Pd(PPh_3)_2Cl_2$ (5.92 mg, 0.0084 mmol) were added to a sealed tube. The tube was evacuated and backfilled with argon (3 cycles). DMF (10.0 mL) and DIPEA (0.44 g, 3.37 mmol) were added by syringe at room temperature. After stirring at 80 ^{o}C overnight, the reaction mixture was diluted with ethyl acetate, washed with water and brine, dried and concentrated. The residue was purified by flash column chromatography on silica gel to afford the

desired SEM protected product (0.34g, yield: 58%). The SEM protective was further removed by $N(Bu)_4F$ in THF (1.0 M) which was refluxed overnight to afford the desired product as yellow solid. (yield: 50%) ^{1}H NMR (400 MHz, d-DMSO), δ 13.45 (s, 1 H), 10.54 (s, 1 H), 8.68 (d, *J* = 2.0 Hz, 1 H), 8.54 (d, *J* = 2.0 Hz, 1 H), 8.21 (d, *J* = 2.0 Hz, 1 H), 8.19 (d, *J* = 1.6 Hz, 1 H), 8.07 (d, *J* = 8.4 Hz, 1 H), 7.92 (dd, *J* = 1.6, 8.0 Hz, 1 H), 7.70 (d, *J* = 8.4 Hz, 1 H), 7.52 (d, *J* = 8.0 Hz, 1 H), 3.56 (s, 1 H), 2.59 (s, 3 H), 2.40-2.34 (m, 9 H), 2.15 (s, 3 H), 1.03-1.00 (m, 4 H); ^{13}C NMR (125 MHz, d-DMSO), δ 164.67, 151.22, 150.91, 146.84, 143.55, 138.14, 132.27, 132.14, 132.02, 131.16, 130.52, 129.85, 127.97, 127.36, 124.29, 123.43, 122.27, 117.21, 112.83, 110.84, 92.06, 88.12, 57.41, 55.97, 54.68, 52.65, 45.66, 20.41, 18.49, 8.12, 7.73; MS (EI): 573 $[M+H]^+$; Purity: 96.62% (t_R 7.10 min).

4-Methyl-3-((3-methyl-1H-pyrazolo[3,4-b]pyridin-5-yl)ethynyl)-N-(4-((4-methylpiperazin-1-yl)methyl)-3-(trifluoromethyl)phenyl)benzamide (**10f**). This compound was synthesized by reacting **14** with **18a** under similar procedure to that of **10g**. Yield: 35%. ^{1}H NMR (400 MHz, d-DMSO), δ 13.50 (s, 1 H), 10.54 (s, 1 H), 8.69 (d, *J* = 2.0 Hz, 1H), 8.52 (d, *J* = 2.0 Hz, 1 H), 8.20 (d, *J* = 2.0 Hz, 1 H), 8.17 (d, *J* = 1.6 Hz, 1 H), 8.06 (d, *J* = 8.4 Hz, 1 H), 7.92 (dd, *J* = 1.6, 8.0 Hz, 1 H), 7.71 (d, *J* = 8.4 Hz, 1 H), 7.52 (d, *J* = 8.0 Hz, 1 H), 3.56 (s, 2 H), 2.59 (s, 3 H), 2.53 (s, 3 H), 2.39 (br, 4 H), 2.33 (br, 4 H), 2.15 (s, 3 H); ^{13}C NMR (125 MHz, d-DMSO), δ 164.76, 151.27, 150.87, 143.62, 141.72, 138.19, 132.57, 132.19, 132.09, 131.22, 130.56, 129.91, 128.03, 127.44, 124.36, 123.51, 122.33, 117.28, 113.61, 110.93, 92.11, 88.16, 57.48, 54.73, 52.69, 45.70, 20.46, 12.11; MS (EI): 547 $[M+H]^+$. Purity: 98.24% (t_R 13.64 min).

4-Methyl-N-(4-((4-methylpiperazin-1-yl)methyl)-3-(trifluoromethyl)phenyl)-3-((3-phenyl-1H-pyrazolo[3,4-b]pyridin-5-yl)ethynyl)benzamide (**10h**). This compound was synthesized by reacting **14** with **18c** under similar procedure to that of **10g**. Yield: 40%. ^{1}H NMR (400 MHz, d-DMSO), δ 10.54 (s, 1 H), 8.82 (d, *J* = 2.0 Hz, 1 H), 8.78 (d, *J* = 1.6 Hz, 1 H), 8.22 (s, 2 H), 8.09-8.06 (m, 3 H), 7.93 (dd, *J* = 2.0, 8.0 Hz, 1 H), 7.71 (d, *J* = 8.8 Hz, 1 H), 7.57-7.52 (m, 3 H), 7.47-7.43 (m, 1 H), 3.56 (s, 2 H), 2.61 (s, 3 H), 2.39 (br, 4 H), 2.34 (br, 4 H), 2.15 (s, 3 H); ^{13}C NMR (125 MHz, d-DMSO), δ 164.68, 151.90,

150.99, 143.63, 143.01, 138.12, 133.10, 132.67, 132.15, 132.04, 131.18, 130.65, 129.87, 128.97, 128.30, 128.03, 127.47, 127.42, 126.61, 125.38, 123.45, 123.20, 122.22, 117.20, 112.22, 111.58, 91.93, 88.56, 57.41, 55.96, 54.68, 52.65, 45.66, 23.01, 20.45, 18.49, 13.40; MS (EI): 609 $[M+H]^+$;Purity: 97.50% (t_R 10.54 min).

3-((3-Methoxy-1H-pyrazolo[3,4-b]pyridin-5-yl)ethynyl)-4-methyl-N-(4-((4-methylpiperazin-1-yl)methyl)-3-(trifluoromethyl)phenyl)benzamide (**10i**). This compound was synthesized by reacting **14** with **20** under similar procedure to that of **10g** except for using TFA in DCM with stirring for 8 hrs at room temperature to remove the PMB protecting group. Yield: 45%. ^{1}H NMR (400 MHz, d-DMSO), δ 10.53 (s, 1 H), 8.68 (s, 1 H), 8.35 (s, 1 H), 8.21 (s, 1 H), 8.17 (s, 1 H), 8.06 (d, J = 8.4 Hz, 1 H), 7.91 (d, J = 7.2 Hz, 1 H), 7.70 (d, J = 8.0 Hz, 1 H), 7.51 (d, J = 7.6 Hz, 1 H), 4.03 (s, 3H), 3.56 (s, 2 H), 2.58 (s, 3 H), 2.39 (br, 8 H), 2.15 (s, 3 H); ^{13}C NMR (125 MHz, d-DMSO), δ 164.70, 154.84, 151.95, 150.93, 143.63, 138.16, 132.14, 132.04, 131.69, 131.18, 130.46, 129.86, 127.99, 127.38, 124.32, 123.47, 122.26, 117.24, 110.44, 103.09, 91.89, 88.19, 57.43, 55.73, 54.70, 52.66, 45.67, 20.40;MS (EI): 563 $[M+H]^+$; Purity: 99.47% (t_R 6.91 min).

3-((1H-indazol-5-yl)ethynyl)-4-methyl-N-(4-((4-methylpiperazin-1-yl)methyl)-3-(trifluoromethyl)phenyl)benzamide **(25a)** This compound can be synthesized by the method similar to **10g** from its corresponding starting material 5-bromo-1H-indazole (**26a**) which was commercially available with **14**. Yield: 43%. ^{1}H NMR (400 MHz, d-DMSO), δ 13.32 (s, 1 H), 10.52 (s, 1 H), 8.22 (s, 1 H), 8.17 (s, 1 H), 8.15 (s, 1 H), 8.07 (s, 2 H), 7.90 (d, J = 7.6 Hz, 1 H), 7.70 (d, J = 8.4 Hz, 1 H), 7.62 (d, J = 8.4 Hz, 1 H), 7.53 (d, J = 9.6 Hz, 1 H), 7.50 (d, J = 8.0 Hz, 1 H), 3.56 (s, 2 H), 2.57 (s, 3 H), 2.38 (br, 4 H), 2.33 (br, 4 H), 2.15 (s, 3 H); ^{13}C NMR (125 MHz, d-DMSO), δ 164.75, 143.47, 138.18, 132.12, 132.03, 131.19, 130.32, 129.85, 128.95, 127.76, 127.38, 124.48, 124.33, 123.47, 122.86, 122.67, 117.24, 113.86, 110.87, 95.08, 85.68, 57.44, 54.70, 52.67, 45.68, 20.41; MS (EI): 532 $[M+H]^+$; Purity: 98.08% (t_R 13.00 min).

4-Methyl-3-((1-methyl-1H-pyrazolo[3,4-b]pyridin-5-yl)ethynyl)-N-(4-((4-methylpiperazin-1-yl)methyl)-3-(trifluoromethyl)phenyl)benzamide (24b) This compound was synthesized by the method similar to **10g** from its corresponding starting material **26b** with **14**. Yield: 53%. ^{1}H NMR (400 MHz, d-DMSO), δ 10.53 (s, 1 H), 8.77 (d, *J* = 1.6 Hz, 1 H), 8.53 (d, *J* = 1.6 Hz, 1 H), 8.22 (s, 1 H), 8.20 (d, *J* = 1.6 Hz, 1 H), 8.19 (d, *J* = 1.6 Hz, 1 H), 8.06 (d, *J* = 8.4 Hz, 1 H), 7.92 (dd, *J* = 1.6, 8.0 Hz, 1 H), 7.70 (d, *J* = 8.4 Hz, 1 H), 7.52 (d, *J* = 8.0 Hz, 1 H), 4.09 (s, 3 H), 3.56 (s, 2 H), 2.59 (s, 3 H), 2.39 (br, 4 H), 2.33 (br, 4 H), 2.15 (s, 3 H); ^{13}C NMR (125 MHz, d-DMSO), δ 164.67, 150.93, 148.65, 143.68, 138.16, 133.30, 132.47, 132.15, 132.06, 131.18, 130.55, 129.91, 127.40, 124.34, 123.47, 122.12, 117.26, 114.57, 111.88, 91.69, 88.52, 57.46, 54.72, 52.68, 45.69, 33.78, 20.41; MS (EI): 547 [M+H] $^{+}$; Purity: 99.44% (t_R 16.93 min).

***3-([1,2,4]Triazolo[1,5-a]pyrimidin-6-ylethynyl)-4-methyl-N-(4-((4-methylpiperazin-1-yl)methyl)-3-(trifluoromethyl)phenyl)benzamide* (25)** This compound was synthesized by the method similar to **10g** from its corresponding starting material **27** with **14**. Yield: 59%. ^{1}H NMR (400 MHz, d-DMSO), δ 10.57 (s, 1 H), 9.87 (d, *J* = 2.0 Hz, 1H), 8.77 (s, 1 H), 8.20 (s, 2 H), 8.05 (d, *J* = 8.4 Hz, 1H), 7.97 (d, *J* = 8.0 Hz, 1 H), 7.71 (d, *J* = 8.4 Hz, 1 H), 7.55 (d, *J* = 8.0 Hz, 1 H), 3.56 (s, 2 H), 2.60 (s, 3 H), 2.39 (br, 4 H), 2.33 (br, 4 H), 2.15 (s, 3 H); ^{13}C NMR (125 MHz, d-DMSO), δ 164.60, 156.97, 156.76, 153.59, 144.12, 139.44, 138.11, 132.25, 132.14, 131.23, 130.93, 130.03, 128.70, 127.42, 127.07, 124.32, 123.50, 121.32, 117.28, 107.65, 91.72, 86.51, 57.45, 54.71, 52.67, 45.68, 20.39; MS (EI): 534 [M+H] $^{+}$; Purity: 99.69% (t_R 8.48 min).

Computational study. The crystal structures of type I conformations of wild-type and Bcr-Abl ^{T315I} mutant were taken from PDB ID 3QRI and 3IK3, and the crystal structures of type II conformations of wild-type and Bcr-Abl ^{T315I} mutant were 2GQG and 2V7A. Hydrogen atoms and charges were added during a brief relaxation performed using the "Protein Preparation Wizard" workflow in Maestro 9.0 (Schrodinger LLC). All HETATM residues and crystal water molecules were removed. After the hydrogen bond network was optimized, the crystal structures were minimized until the RMSD between

the minimized structure and the starting structure reached 0.3 Å with OPLS 2005 force field. The grid-enclosing box was placed on the centroid of the binding ligand in the optimized crystal structure as described above and defined to enclose residues located within 14.0 Å of the ligand binding site, and a scaling factor of 1.0 was set to van der Waals (VDW) radii of those receptor atoms with partial atomic charges of less than 0.25. The structure of **10a** was drawn using the Builder tool and then optimized with Ligprep module in Maestro. Standard precision (SP) approach of Glide was adopted to dock GZD824 to Bcr-Abl with the default parameters, and the top-ranking pose was retained as the reasonable binding pose.

Cells and reagents. The leukemia cell lines (K562, KU812, SUP-B15, U-937, MOLT4) were purchased from ATCC and maintained as recommended by ATCC (Manassas, USA). Imatinib, dasatinib and nilotinib were purchased from Biocompounds Pharmaceutical Inc. (Shanghai,China). CCK-8 was purchased from Dojindo Molecular Technologies Inc (Kumamoto, JAPAN). Dimethyl Sulfoxide (DMSO) and Cremophor were purchased from Sigma-Aldrich (Dorset, USA). D-luciferin potassium was purchased from Gold Biotechnology (St. Louis, USA). Antibodies against Abl, p-Abl, Crkl, p-Crkl, STAT5, p-STAT5, respectively, were all purchase from Cell Signaling Technology Inc (Danvers, USA)

Stably transformed Ba/F3 cells. The Ba/F3 cell lines stably-expressing native Bcr-Abl or various Bcr-Abl mutants were self-established by following similar procedures to those described by Nikolas von Bubnoff.[50] Briefly, wild-type Bcr-Abl p210 was cloned into pCDNA3.1(+) (Invitrogen, Carlsbad, USA). Point mutations were introduced to pCDNA3.1(+) Bcr-Abl using the QuickChange XL Site-Directed Mutagenesis Kit (Stratagene, La Jolla, USA). Ba/F3 cells were transfected with the constructs using Transfected Cells Cloning Kit (Stem Cell Technologies, Vancouver, Canada) by electroporation. Stable lines were selected using Amaxa Cell Line Nucleofector Kit V (Lonza, Cologne,Germany) with G418 (Merck, Whitehouse Station, USA) and withdrawal of Interleukin-3 (IL-3, R&D). All of Ba/F3 stable cell lines were verified by monitoring both DNA sequences through DNA sequencing and protein

expression levels of the corresponding Bcr-Abl mutants through western blotting analysis. The IC_{50} values of imatinib, nilotinib and dasatinib were also utilized as reference for clone selection. For the Ba/F3 cells co-expressing Bcr-Abl ^{T315I} and firefly luciferase, Ba/F3 stable lines expressing Bcr-Abl ^{T315I} were further stably- transfected with pBABE-Luc (A gift from Dr Biliang Zhang). Parental Ba/F3 cells were cultured in RPMI 1640 supplemented with 10% Fetal Bovine Serum (FBS) and (Il-3, 10ng/ml), while all Bcr-Abl-transformed Ba/F3 stable cell lines were cultured in the similar medium except without IL-3. Imatinib-resistant K562 cells which expressed Bcr-Abl ^{Q252H} were self-established. Briefly, K562 cells were treated with a range of concentrations of imatinib (from 0.1 μM to 5 μM) over a 3 month period. Single clones were then selected and identified through DNA sequencing and their response to imatinib, nilotinib and dasatinib were monitored as an internal reference.

Active-site dependent competition binding assay- Kinomescan screening. The binding activities of **10a** with native Abl or Abl-mutants were analyzed by KINOME *scan*™ system conducted by Ambit Bioscience (San Diego, USA). Briefly, kinases were tagged with DNA. The ligands were biotinylated and immobilized to streptavidin-coated beads. The binding reactions were assembled by incubating DNA-tagged kinases, immobilized ligands and test compounds in binding reactions (20% SeaBlock, 0.17×PBS, 0.05% tween-20, 6 mM DTT) for 1.0 hour at room temperature. The affinity beads were washed with washing buffer (1×PBS, 0.05% Tween-20) first and then elution buffer (1×PBS, 0.05% Tween 20, 0.5 μM non-biotinylated affinity ligands). The kinase concentration in the eluate was determined by quantitative PCR of the DNA tagged to the kinase. The ability of the test compound to bind to the kinase was evaluated with percent control (%) as (Test compound signal – positive control signal)/ Negative control signal – positive control signal) × 100%. Negative control is DMSO control (100% Ctrl) and positive control is control compound (0 % Ctrl).

FRET-based Z'-Lyte assay detecting peptide substrate phosphorylation. The kinases are commercially purchased from Invitrogen (USA). The catalog numbers of kinases ABL1, ABL1(E255K), ABL1 (G250E), ABL1(T315I), and ABL1(Y253F) are P3049, PV3864, PV3865,

PV3866, and PV3863, respectively. All of them are Full-length Human recombinant protein expressed in insect cells with Histidine-tagged. Inhibition activities of inhibitors against Abl1 and its mutants were performed in 384-well plates using the FRET-based Z'-Lyte assay system according to the manufacturer's instructions (Invitrogen, Carlsbad, USA). Briefly, the kinase substrate was diluted into 5μL 1X kinase reaction buffer; and the kinase was added. Compounds (10 nL) with indicated concentrations were then delivered to the reaction by using Echo liquid handler and the mixture was incubated for 30 minutes at room temperature. Then 5 μL of 2X ATP solution was added to initiate the reaction and the mixture was further incubated for 2 hour at room temperature. The resulting reactions contained 10 μM (for wild-type Abl1, and mutants Y253F, Q252H, M351T and H396P) or 5 μM (for mutants E255K, G250E, T315I) of ATP, 2μM of Tyr2 Peptide substrate in 50 mM HEPES (PH 7.5), 0.01% BRIJ-35, 10 mM MgCl2, 1 mM EGTA, 0.0247 μg/ml Abl1 and inhibitors as appropriate. Then, 5μL development reagent was added and the mixture was incubated for 2 hours at room temperature incubation before 5 μL of stop solution was added. Fluorescence signal ratio of 445 nm (Coumarin)/520 nm (fluorescin) was examined on EnVision Multilabel Reader (Perkin Elmer, Inc.). The data were analyzed using Graphpad Prism5 (Graphpad Software ,Inc). The data was the mean value of 3 experiments.

Antiproliferation assay using Cell Counting Kit (CCK-8). Cells in the logarithmic phase were plated in 96-well culture dishes (~3000 cells/ well). 24 hours later, cells were treated with the corresponding compounds or vehicle control at the indicated concentration for 72 hours. CCK-8 was added into the 96- well plates (10 μl / well) and incubated with the cells for 3 hours. OD450 and OD650 were determined by a micro-plate reader. Absorbance rate (A) for each well was calculated as OD450-OD650. The cell viability rate for each well was calculated as V% =(As-Ac)/(Ab-Ac)×100% and the data were further analyzed using Graphpad Prism5 (Graphpad Software ,Inc.) The data was the mean value of the 3 experiments. As, Absorbance rate of the test compound well; Ac, absorbance rate of the well without either cell or test compound; Ab, absorbance rate of the well with cell and vehicle control.

Western blot analysis. The western blot analysis was carried out by following the protocol described before. [51] Briefly, after the indicated treatment, cell lysates were collected dissolving cells in 1×SDS sample lysis buffer. After being sonicated and boiled, the supernatant of cell lysate were used for western blot analysis. Cell lysates were loaded to 8-12% SDS-PAGE and separated by electrophoresis. Separated proteins were then electrically transfered to a PVDF film. After being blocked with 1×TBS containing 0.1% Tween-20 and 5% non-fat milk, the film was incubated with corresponding primary antibody followed by HRP-conjugated secondary antibody. And the protein lanes were visualized using ECL Western Blotting Detection Kit (GE healthcare, Piscataway, USA).

Animal studies. Male BALB/c or SCID nude mice were purchased from Vital River Laboratory Animal Technology Inc (Beijing, China). All animal studies were approved by the Institutional Animal Use and Care Committee of Guangzhou Institute of Biomedicine and Health, Chinese Academy of Science.

Mice xenograft or allograft tumor models using K562 and transformed Ba/F3 cells expressing native Bcr-Abl or Bcr-Abl mutants. K562 cells or Ba/F3 cells expressing native Bcr-Abl or Bcr-Abl mutants were resuspended in normal saline (NS) solution (2.5×10^7 cell /ml). 0.2 ml of cell suspension was injected subcutaneously into the right flank of each mouse. Mice were randomly grouped based on the tumor volume when the mean tumor volume reached 100-200 mm^3. Compound **10a** and Imatinib were dissolved in a vehicle containing 1% DMSO, 22.5% Cremophor, 7.5% ethanol and 69% normal saline (NS). Mice were treated for the 14 consecutive days once daily by oral gavage with **10a** (at the indicated doses), Imatinib (50mg/kg) and vehicle, respectively. Tumor volume and body weight were monitored once every 2 days. Tumor volume was calculated as the $L \times W^2/2$ (L and W are the length and width of the tumor, respectively).

Mice allograft model using Ba/F3 cells expressing Bcr-Abl^{T315I}. Ba/F3 cells co-expressing BCR-ABL^{T315I} and firefly luciferase were resuspended innormal saline (NS) solution and intravenously injected into SCID nude mice (2×10^6 cells/ 0.1 ml). At 5-7 days after inoculation, proliferation of the

Ba/F3 cells *in vivo* in mice was monitored through *in vivo* fluorescence imaging with XENOGEN IVIS-200 System (University of Maryland Greenebaum Cancer Center, Baltimore, USA). Briefly, Mice were intraperitoneally injected with 150 µl of D-luciferin potassium solution (150mg/m in PBS) and anesthetized with halothane. 5 minutes later, the *in vivo* fluorescence images of the mice were taken. Mice were then randomized to treatment groups based on the magnitude of the fluorescence signal. Grouped mice were dosed once daily through oral gavage for 10 consecutive days with **10a** of indicated doses or Imatinib (100mg/kg), or vehicle (as described above). The body weight was recorded once every two days. Proliferation of the Ba/F3 cells were monitored by *in vivo* fluorescence imaging at the indicated time point post dose. Survival days of the mice were recorded and survival data were analyzed with Kaplan-Meier method using software SPSS13.0.

Statistics. For the *in vivo* xenograft and *in vivo* allograft tumor models, the unpaired Student's T test was used to assess differences of the tumor progression between the groups receiving **10a** treatment or Imatinib treatment and vehicle-treated control groups. The survival difference among **10a**/Imatinib-treated groups and vehicle-treated group was assessed by one way ANOVA log-rank test using Kaplan Meier method of SPSS13.0. Difference with $P < 0.05$ and $P < 0.01$ were considered significant and very significant, and marked as* and **, respectively.

SUPPORTING INFORMATION

Chemical data of the final compounds, synthesis of key intermediates, and additional biological data can be obtained in supporting information. This material is available free of charge *via* the Internet at http://pubs.acs.org.

ABBREVIATION: For amino acids: E, glutamic acid; G, Glycine; H, histidine; K, lysine; P, praline; S, serine; T, threonine; M, methionine; I, isoleucine; L, leucine; R, arginine; E, glutamic acid; Y, tyrosine; V, valine; A, alanine; Q, glutamine; F, phenylalanine; D, aspartic acid; Abl, Abelson murine leukemia viral oncogene; AIBN, azodiisobutyronitrile; ATP, adenosine triphosphate; Bcr, breakpoint

cluster region; Boc, tert-butoxycarbonyl; CML, chronic myelogenous leukaemia; DCM, dichloromethane; DFG, Asp-Phe-Gly; DMF, *N, N*- imethylformamide; DMSO, dimethyl sulfoxide; NBS, *N*-bromosuccinimide; rt, room temperature; TFA, trifluoroacetic acid; THF, tetrahydrofuran; WT, wild-type; SEM-Cl, 2-(trimethylsilyl)ethoxymethyl chloride; NIS, *N*-iodosuccinimide; ALL, acute lymphocyte leukemia; Ar, argon; DIPEA, *N, N*-diisopropylethylamine, FRET, Fluorescence resonance energy transfer; DDR, discoidin domain receptor; FGFR, fibroblast growth factor receptor; Flt3, FMS-like tyrosine kinase-3; PDGFR, platelet derived growth factor receptor; RET, rearranged during transfection kinase; Src, sarcoma; Tie, tyrosine kinase with immunoglobulin and EGF-like domains; Raf, rapidly accelerated fibrosarcoma; ADME, absorption, distribution, metabolism, and excretion; CYP, cytochrome P-450; hERG, human ether-a-go-go related gene.

ACKNOWLEDGMENT

We thank National Basic Research Program of China (# 2010CB529706), Major Projects in National Science and Technology "Creation of major new drugs" (# 2013ZX0910204), National Natural Science Foundation (# 21072192, 21102146), key Project on Innovative Drug of Guangdong province (# 2011A080501013), Key Project on Innovative Drug of Guangzhou City (# 2009Z1-E911, 2010J-E551, 12C34061592) and the grant from Chinese Academy of Sciences (CAS) for their financial support. We also thank Dr. Jeff Snail (the University of Auckland, New Zealand) for the help on preparation of the paper. Prof. Honglin Li (East China University of Science and Technology) was also acknowledged for the help on the docking studies.

REFERENCES

1. Druker, B. J.; Sawyers, C. L.; Kantarjian, H.; Resta, D. J.; Reese, S. F.; Ford, J. M.; Capdeville, R.; Talpaz, M. Activities of a specific inhibitor of the Bcr-Abl tyrosine kinase in the blast crisis of chronic myeloid leukemia and acute lymphoblastic leukemia with the Philadelphia chromosome. *N. Engl. J. Med.* **2001**, *344*, 1038-1042.

2. Druker, B. J.; Talpaz, M.; Resta, D. J.; Peng, B.; Buchdunger, E.; Ford, J. M.; Lydon, N. B.; Kantarjian, H.; Capdeville, R.; Ohno-Jones, S.; Sawyers, C. L. Efficacy and safety of a specific inhibitor of the Bcr-Abl tyrosine kinase in chronic myeloid leukemia. *N. Engl. J. Med.* **2001**, *344*, 1031-1037.

3. Mauro, M. J.; and Druker, B. J. STI571: Targeting BCR-ABL as therapy for CML. *Oncologist* **2001**, *6*, 233-238.

4. Kantarjian, H.; Sawyers, C.; Hochhaus, A.; Guilhot, F.; Schiffer, C.; Gambacorti-Passerini, C.; Niederwieser, D.; Resta, D.; Capdeville, R.; Zoellner, U.; Talpaz, M.; Druker, B. Hematologic and cytogenetic responses to imatinib mesylate in chronic myelogenous leukemia. *N. Engl. J. Med.* **2002**, *346*, 645-652.

5. Druker, B. J.; Guilhot, F.; O'Brien, S. G.; Gathmann, I.; Kantarjian, H.; Gattermann, N.; Deininger, M. W.; Silver, R. T.; Goldman, J. M.; Stone, R. M.; Cervantes, F.; Hochhaus, A.; Powell, B. L.; Gabrilove, J. L.; Rousselot, P.; Reiffers, J.; Cornelissen, J. J.; Hughes, T.; Agis, H.; Fischer, T.; Verhoef, G.; Shepherd, J.; Saglio, G.; Gratwohl, A.; Nielsen, J. L.; Radich, J. P.; Simonsson, B.; Taylor, K.;, Baccarani, M.; So C, Letvak, L.; Larson, R. A. Five-year follow-up of patients receiving imatinib for chronic myeloid leukemia. *N. Engl. J. Med.* **2006**, *355*, 2408-2417.

6. Deininger, M.; O'Brien, S. G.; Guilhot, F.; M Goldman, J. M.; Hochhaus, A.; Hughes, T. P.; Radich, J. P.; Hatfield, A. K.; Mone, M.; Filian, J.; Reynolds, J.; Gathmann, I.; Larson, R. A.; Druker, B. J. International randomized study of interferon vs STI571(IRIS) 8-year follow up: consistainded survival and low risk for progression or events in patients with newly diagnosed chronic myeloid leukemia in chronic phase(CML-CP) treated with imatinib. *ASH Ann. Meeting Abstr.* **2009**, *114*, 1126.

7. O'Hare, T.; Eide, C. A.; Deininger, M. W. N. Bcr-Abl kinase domain mutations, drug resistance, and the road to a cure for chronic myeloid leukemia. *Blood* **2007**, *110*, 2242-2249.

8. Shah, N. P.; Nicoll1, J. M.; Nagar, B.; Gorre, M. E.; Paquette, R. L.; Kuriyan, J.; Sawyers, C. L. Multiple BCR-ABL-kinase domain mutations confer polyclonal resistance to the tyrosine kinase

inhibitor imatinib (STI571) in chronic phase and blast crisis chronic myeloid leukemia. *Cancer Cell* **2002**, *2*, 117-125.

9. O'Hare, T.; Walters, D. K.; Stoffregen, E. P.; Jia, P.; Manley, P. W.; Mestan, J.; Cowan-Jacob, S. W.; Lee, F. Y.; Heinrich, M. C.; Deininger, M. W. N.; Druker, D. J. *In vitro* Activity of Bcr-Abl Inhibitors AMN107 and BMS-354825 against Clinically Relevant Imatinib-Resistant Abl Kinase Domain Mutants. *Cancer Res.* **2005**, *65*, 4500-4505.

10. (a) Weisberg, E.; Manley, P. W.; Breitenstein, W.; Brüggen, J.; Cowan-Jacob, S. W.; Ray1, A.; Huntly, B.; Fabbro, D.; Fendrich, G.; Hall-Meyers, E.; Kung, A. L.; Mestan, J.; Daley, G. Q.; Callahan, L.; Catley, L.; Cavazza1, C.; Mohammed, A.; Neuberg, D.; Wright, R. D.; Gilliland, D. G.; Griffin, J. D. Characterization of AMN107, a selective inhibitor of wild-type and mutant Bcr-Abl. *Cancer Cell* **2005**, *7*, 129-141; (b) Kantarjian, H. M.; Giles, F.; Gattermann, N.; Bhalla, K.; Alimena, G.; Palandri, F.; Ossenkoppele, G.. J.; Nicolini, F. E.; O'Brien, S. G.; Litzow, M.; Bhatia, R.; Cervantes, F.; Haque, A.; Shou, Y.; Resta, D. J.; Weitzman, A.; Hochhaus, A.; le Coutre, P. Nilotinib (formerly AMN 107), a highly selective Bcr-Abl tyrosine kinase inhibitor, is effective in patients with Philadelphis chromosome positive chronic myelogenous leukemia in chronic phase following imatinib resistance and intolerance. *Blood* **2007**, *110*, 3540-3546.

11. (a) Shah, N. P.; Tran, C.; Lee, F.; Y.; Chen, P.; Norris, D. and Sawyers, C. L. Overridering imatinib resistance with novel ABL kinase inhibitor. *Science* **2004**, *305*, 399-401; (b) Quintas-Cardama, A.; Kantarjian, H.; Jones, D.; Nicaise, C.; O'Brien, S.; Giles, F.; Talpaz, M. and Cortes, J. Dasatinib (BMS-354825) is active in Philadelphia chromosome-positive chronic myelogenous leukemia after imatinib and nilotinib (AMN107) therapy failure. *Blood* **2007**, *109*, 497-499.

12. Kimura, S.; Naito, H.; Segawa, H.; Kuroda, J.; Yuasa, T.; Sato, K.; Yokota, A.; Kamitsuji, Y.; Kawata, E.; Ashihara, E.; Nakaya, Y.; Naruoka, H.; Wakayama, T.; Nasu, K.; Asaki, T.; Niwa, T.;

Hirabayashi, K.; Maekawa, T. NS-187, a potent and selective dual Bcr-Abl/Lyn tyrosine kinase inhibitor, is a novel agent for imatinib-resistant leukemia. *Blood* **2005**, *106*, 3948-3954.

13. Puttini, M.; Coluccia, A. M.; Boschelli, F.; Cleris, L.; Marchesi, E.; Donella-Deana, A.; Ahmed, S.; Redaelli, S.; Piazza, R.; Magistroni, V.; Andreoni, F.; Scapozza, L.; Formelli, F.; Gambacorti-Passerini, C. *In vitro* and *in vivo* activity of SKI-606, a novel Src-Abl inhibitor, against imatinib-resistant Bcr-Abl+ neoplastic cells. *Cancer Res.* **2006**, *66*, 11314-11322.

14. Bradeen, H. A.; Eide, C. A.; O'Hare, T.; Johnson, K. J.; Willis, S. G.; Lee, F. Y.; Druker, B. J.; Deininger, M. W. Comparison of imatinib, dasatinib (BMD-354825), and nilotinib (AMN107) in an n-ehtyl-n-nitrosourea (ENU)-based mutagenesis screen: high efficacy of drug combinations. *Blood* **2006,** *108*, 2332-2338.

15. Burgess, M. R.; Skaggs, B. J.; Shah, N. P.; Lee, F. Y.; Sawyers, C. L. Comparative analysis of two clinically active BCR-ABL kinase inhibitors reveals the role of conformation-specific binding in resistance. *Proc. Natl. Acad. Sci. USA.* **2005**, *102*, 3395-3400.

16. Roychowdhury, S.; Talpaz, M. Managing resistance in chronic myeloid leukemia. *Blood Rev.* **2011**, *25*, 279-290.

17. Schindler, T.; Bornmann, W.; Pellicena, P.; Miller, W. T.; Clarkson, B.; Kuriyan, J. Structural mechanism for STI-571 inhibition of abelson tyrosine kianse. *Science* **2000**, *289*, 1948-1942.

18. Tokarski, J. S.; Newitt, J. A.; Chang, C. Y.; Cheng, J. D.; Wittekind, M.; Kiefer, S. E.; Kish, K.; Lee, F. Y.; Borzillerri, R.; Lombardo, L. J.; Xie D.; Zhang Y.; and Klei, H. E. The structure of Dasatinib, (BMS 354825) bound to activated ABL kinase domain elucidates its inhibitory activity against imatinib resistant ABL mutants. *Cancer Res.* **2006**, *66*, 5790-5797.

19. Zhou, T.; Parillon, L.; Li, F.; Wang, Y.; Keats, J.; Lamore, S.; Xu, Q.; Shakespeare, W.; Dalgarno, D.; Zhu, X. Crystal strucrure of the T315I mutant of Abl kinase. *Chem. Biol. Drug Des.* **2007**, *70*, 171-181.

20. Gorre, M. E., Mohammed, M.; Ellwood, K.; Hsu, N.; Paquette, R.; Rao, P. N.; Sawyers, C. L. Clinical resistance to STI571 cancer therapy caused by Bcr-Abl gene mutation or amplification. *Science* **2001**, *293*, 876-880.

21. Azam, M.; Latek, R.R.; and Daley, G. Q. Mechanism of autoinhibition and STI-571/imatinib resistance revealed by mutagenesis of BCR-ABL. *Cell* **2003**, *112*, 831-843.

22. Azam, M.; Seeliger, M. A.; Gray, N. S.; Kuriyan, J.; Daley, G. Q. Activation of tyrosine kinases by mutations of the gatekeeper threonine. *Nat. Srtuct. Mol. Bio.* **2008**, 15, 1109-1118.

23. Cortes, J.; Jabbour, E.; Kantarjian, H.; Yin, C. C.; Shan, J.; O'Brien, S.; Garcia-Manero, G.; Giles, F.; Breeden, M.; Reeves, N.; Wierda, W. G..; Jones, D.Dynamics of BCR-ABL kinase domain mutations in chronic myeloid leukemia after sequential treatment with multiple tyrosine kinase inhibitors. *Blood* **2007**, *110*, 4005-4011.

24. Shah, N. P.; Skaggs, B. J.; Branford, S.; Hughes, T. P.; Nicoll, J. M.; Paquette, R. L.; Sawyers, C. L. Sequential ABL kinase inhibitor therapy selects for compound drug resistant BCR ABL mutations with altered oncogenic potency. *J. Clin. Invest.* **2007**, *117*, 2562-2569.

25. Soverini, S.; Martinelli, G.; Colarossi, S.; Gnani, A.; Castagnetti, F.; Rosti, G.; Bosi, C.; Paolini, S.; Rondoni, M.; Piccaluga, P. P.; Palandri, F.; Giannoulia, P.; Marzocchi, G.; Luatti, S.; Testoni, N. and Iacobucci, I. Presence or the emergence of a F317L Bcr-Abl mutation may be associated with resistance to dasatinib in Philadelphia chromosome-positive leukemia. *J. Clin. Oncol.* **2006**, *24*, e51-52.

26. Examples see: (a) Schenone, S.; Bruno, O.; Radi, M.; Botta, M. New insights into small-molecule inhibitors of Bcr-Abl. *Med. Res. Rev.* **2011**, *31*, 1-41; (b) Choi, H. G.; Zhang, J.; Weisberg, E.; Griffin, J.

D.; Sim, T.; Gray, N. S. Development of 'DFG-out' inhibitors of gatekeeper mutant kinases. *Bioorg. Med. Chem. Lett.* **2012**, *22*, 5297-5302; (c) Zhou, T.; Parillon, L.; Li, F.; Wang, Y.; Keats, J.; Lamore, S.; Xu, Q.; Shakespeare, W.; Dalgarno, D.; Zhu, X. Crystal structure of the T315I mutant of Abl kinase. *Chem. Biol. Drug. Des.* **2007**, *70*, 171-181; (d) Cao, J. G.; Fine, R.; Gritzen, C.; Hood, J.; Kang, X. S.; Klebansky, B.; Lohse, D.; Mak, C. C.; McPherson, A.; Noronha, G.; Palankl, M. S. S.; Pathak, V. P.; Renick, J.; Solla, R.; Zenga, B. Q.; Zhu, H. The design and preliminary structure-activity relationship studies of benzotriazines as potent inhibitors of Abl and Abl-T3151 enzymes. *Bioorg. Med. Chem. Lett.* **2007**, *17*, 5812-5818; (e) Gumireddy, K.; Baker, S. J.; Cosenza, S. C.; John, P.; Kang, A. D.; Robell, K. A.; Reddy, M. V.; Reddy, E. P. A non-ATP-competitive inhibitor of BCR-ABL overrides imatinib resistance. *Proc. Natl. Acad. Sci. USA* **2005**, *102*, 1992-1999; (f) Adrian, F. J.; Ding, Q.; Sim, T.; Velentza, A.; Sloan, C.; Liu, Y.; Zhang, G.; Hur, W.; Ding, S.; Manley, P.; Mestan, J.; Fabbro, D.; Gray, N. S. Allosteric inhibitors of Bcr-abl-dependent cell proliferation. *Nat. Chem. Biol.* **2006**, *2*, 95-102; (g) Zhang, J.; Adrian, F. J.; Jahnke, W.; Cowan-Jacob, S. W.; Li, A. G.; Iacob, R. E.; Sim, T.; Powers, J.; Dierks, C.; Sun, F.; Guo, G. R.; Ding, Q.; Okram, B.; Choi, Y.; Wojciechowski, A.; Deng, X.; Liu, G.; Fendrich, G.; Strauss, A.; Vajpai, N.; Grzesiek, S.; Tuntland, T.; Liu, Y.; Bursulaya, B.; Azam, M.; Manley, P. W.; Engen, J. R.; Daley, G. Q.; Warmuth, M.; Gray, N. S. Targeting Bcr-Abl by combining allosteric with ATP-binding-site inhibitors. *Nature* **2010**, *463*, 501-506; (h) Arioli, F.; Borrelli, S.; Colombo, F.; Falchi, F.; Filipp, I.; Crespan, E.;Naldini, A.; Scalia, G.; Dr. Alessandra Silvani, A.; Maga, G.; Carraro, F.; Maurizio Botta, M.; Passarella,D. N-[2-Methyl-5-(triazol-1-yl)phenyl]pyrimidin-2-amine as a Scaffold for the Synthesis of Inhibitors of Bcr-Abl. *ChemMedChem* **2011**, *11*, 2009-2018.

27. (a) Giles, F. J.; Cortes, J.; Jones, D.; Bergstrom, D.; Kantarjian, H.; Freedman, S. J. MK-0457, a novel kinase inhibitor, is active in patients with chronic myeloid leukemia or acture lymphocytic leukemia with the T315I BCR-ABL mutation. *Blood* **2007**, *109*, 500-502; (b) Okabe, S.; Tauchi, T.; Ohyashiki, J. H.; Ohyashiki, K. Mechanism of MK-0457 efficacy against BCR–ABL positive leukemia cells. *Biochem. Biophy. Res. Commun.* **2009**, *380*, 775-779.

28. Gontarewicz, A.; Balabanov, S.; Keller, G.; Colombo, R.; Graziano, A.; Pesenti, E.; Benten, D.; Bokemeyer, C.; Fiedler, W.; Moll, J.; Brümmendorf, T. H. Simultaneous targeting of Aurora kinases and Bcr-Abl kinase by the small molecule inhibitor PHA-739358 is effective against imatinib-resistane Bcr-Abl mutations including T315I. *Blood* **2008**, *111*, 4355-4364.

29. Tanaka, R.; Squires, M. S.; Kimura, S.; Yokota, A.; Nagao, R.; Yamauchi, T.; Takeuchi, M.; Yao, H.; Reule, M.; Smyth, T.; Lyons, J. F.; Thompson, N. T.; Ashihara, E.; Ottmann, O. G.; Maekawa, T. Activity of the multitargeted kinase inhibitor, AT9283, in imatinib-resistant BCR-ABL–positive leukemic cells. *Blood* **2010**, *116*, 2089-2095.

30. Shah, N.P.; Kasap, C.; Paquette, R; Cortes, J.; Pinilla, J.; Talpaz, M., Bui, L.A.; Clary, D.O. Targeting Drug-Resistant CML and Ph+ All with the Spectrum Selective Protein Kinase Inhibitor XL228. 49th ASH Annual Meeting, December 8-11, 2007, Atlanta, Georgia, Abstract 474.

31. Noronha, G.;, Cao, J.; Chow, C.P.; Dneprovskaia, E.; Fine, R.M., Hood, J., Kang, X.; Klebansky, B.; Lohse, D.; Mak, C.C.; McPherson, A.; Palanki, M.S.; Pathak,V.P.; Renick, J.; Soll, R.; Zeng, B. Inhibitors of ABL and the ABL-T315I mutation. *Curr. Top. Med. Chem.* **2008**, *8*, 905-921.

32. Lu, X.; Cai, Q.; Ding, K. Recent Developments in the Third Generation Inhibitors of Bcr-Abl for Overriding T315I mutation. *Curr. Med. Chem.* **2011**, *18*, 2146-2157.

33. Bikker, J. A.; Brooijmans, N.; Wissner, A. and Mansour, T. S. Kinase Domain Mutations in Cancer: Implications for Small Molecule Drug Design Strategies. *J. Med. Chem.* **2009**, *52*, 1493–1509

34. (a) O'Hare, T.; Shakespeare, W. C.; Zhu, X.; Eide, C. A.; Rivera, V. M.; Wang, F.; Adrian, L. T.; Zhou, T.; Huang, W. S.; Xu, Q.; Metcalf, C. A. III.; Tyner, J. W.; Loriaux, M. M.; Corbin, A. S.; Wardwell, S.; Ning, Y.; Keats, J. A.; Wang, Y.; Sundaramoorthi, R.; Thomas, M.; Zhou, D.; Snodgrass, J.; Commodore, L.; Sawyer, T. K.; Dalgarno, D. C.; Deininger, M. W.; Druker, B. J.; Clackson, T. AP24534, a pan-BCR-ABL inhibitor for chronic myeloid leukemia, potently inhibits the T315I mutant and overcone mutation-based resistance. *Cancer Cell* **2009**, *16*, 401-412; (b) Zhou, T.; Commodore, L.;

Huang, W. S.; Wang, Y.; Thomas, M.; Keats, J.; Xu, Q.; Rivera, V. M.; Shakespeare, W. C.; Clackson, T.; Dalgarno, D. C.; Zhu, X. Structural mechanism of the pan-BCR-ABL inhibitor ponatinib (AP24534): lessons for overcoming kinase inhibitor resistance. *Chem. Biol. Drug Des.* **2011**, *77*, 1-11; (c) Huang, W.-S.; Metcalf, C. A.; Sundaramoorthi, R.; Wang, Y.; Zou, D.; Thomas, R. M.; Zhu, X.; Cai, L.; Wen, D.; Liu, S.; Romero, J.; Qi, J.; Chen, I.; Banda, G.; Lentini, S. P.; Das, S.; Xu, Q.; Keats, J.; Wang, F.; Wardwell, S.; Ning, Y.; Snodgrass, J. T.; Broudy, M. I.; Russian, K.; Zhou, T.; Commodore, L.; Narasimhan, N. I.; Mohemmad, Q. K.; Iuliucci, J.; Rivera, V. M.; Dalgarno, D. C.; Sawyer, T. K.; Clackson, T. and Shakespeare, W. C. Discovery of 3-[2-(Imidazo[1,2-b]pyridazin-3-yl)ethynyl] -4-methyl-N-{4-[(4-methylpiperazin-1-yl) methyl]-3-(trifluoromethyl)phenyl}benzamide (AP24534), a Potent, Orally Active Pan-Inhibitor of Breakpoint Cluster Region-Abelson (BCR-ABL) Kinase Including the T315I Gatekeeper Mutant. *J. Med. Chem.*, **2010**, *53*, 4701–4719.

35. (a) Chan, W. W.; Wise, S. C.; Kaufman, M. D.; Ahn, Y. M.; Ensinger, C. L.; Haack, T.; Hood, M. M.; Jones, J.; Lord, J. W.; Lu, W. P.; Miller, D.; Patt, W. C.; Smith, B. D.; Petillo, P. A.; Rutkoski, T. J.; Telikepalli, H.; Vogeti, L.; Yao, T.; Chun, L.; Clark, R.; Evangelista, P.; Gavrilescu, L. C.; Lazarides, K.; Zaleskas, V. M.; Stewart, L. J.; Van Etten, R. A.; Flynn, D. L. Conformational control inhibition of the BCR-ABL1 tyrosine kinase, including the gatekeeper T315I mutant, by switch-control inhibitior DCC-2036. *Cancer Cell* **2011**, *19*, 556-568; (b) Eide, C. A.; Adrian, L. T.; Tyner, J. W.; Mac Partlin, M.; Anderson, D. J.; Wise, S. C.; Smith, B. D.; Petillo, P. A.; Flynn, D. L.; Deininger, M. W.; O'Hare, T.; Druker, B. J. The ABL switch control inhibitor DCC-2036 is active against the chronic meloid leukemia mutant BCR-ABL T315I and exhibits a narrow resistance profile. *Cancer Res.* **2011**, *71*, 3189-3195.

36. a) Wenglowsky, S.; Ren, L.; Ahrendt, K. A.; Laird, E. R.; Aliagas, I.; Alicke, B.; Buckmelter, A. J.; Choo, E. F.; Dinkel, V.; Feng, B.; Gloor, S. L.; Gould, Gross, S.; Gunzner-Toste, J.; Hansen, J. D.; Hatzivassiliou, G.; Liu, B.; Malesky, K.; Mathieu, S.; Newhouse, B.; Raddatz, N. J.; Ran, Y.; Rana, S.; Randolph, N.; Risom, T.; Rudolph, J.; Savage, S.; Selby, L. T.; Shrag, M.; Song, K.; Sturgis, H. L.;

Voegtli, W. C.; Wen, Z.; Willis, B. S.; Woessner, R. D.; Wu, W. I.; Young, W. B. and Grina, J. Pyrazolopyridine Inhibitors of B-Raf^{V600E}. Part 1: The Development of Selective, Orally Bioavailable, and Efficacious Inhibitors. *ACS Med. Chem. Lett.* **2011**, 2, 342-347. b) Wenglowsky, S.; Ahrendt, K. A.; Buckmelter, A. J.; Feng, B.; Gloor, S. L.; Gradl, S.; Grina, J.; Hansen, J. D.; Laird, E. R.; Lunghofer, P.; Mathieu, S.; Moreno, D.; Newhouse, B.; Ren, L.; Risom, T.; Rudolph, J.; Seo, J.; Sturgis, H. L.; Voegtli, W. C.; Wen, Z. Pyrazolopyridine inhibitors of B-Raf^{V600E}. Part 2: Structure–activity relationships. *Bioorg. Med. Chem. Lett.* **2011**, 21, 5533-5537. c) Wenglowsky, S.; Moreno, D.; Laird, E. R.; Gloor, S. L.; Ren, L.; Risom, T.; Rudolph, J.; Sturgis, H. L.; Voegtli, W. C. Pyrazolopyridine inhibitors of B-Raf^{V600E}. Part 4: Rational design and kinase selectivity profile of cell potent type II inhibitors. *Bioorg. Med. Chem. Lett.* **2012**, 22, 6237–6241. d) Li, Y.; Shen, M.; Zhang, Z.; Luo, J.; Pan, X.; Lu, X.; Long, H.; Wen, D.; Zhang, F.; Leng, F.; Li, Y.; Tu, Z.; Ren, X.; and Ding, K. Design, Synthesis, and Biological Evaluation of 3-(1H-1,2,3-Triazol-1-yl)benzamide Derivatives as Potent Pan Bcr-Abl Inhibitors Including the Threonine315→Isoleucine315 Mutant. *J. Med. Chem.*, **2012**, *55*, 10033–10046.

37. Chinchilla, R.; Najera, C. The Sonogashira reaction: a booming methodology in synthetic organic chemistry. *Chem. Rev.* **2007,** *10*, 874-922.

38. Chang, S.; Zhang, L.; Xu, S.; Luo, J.; Lu, X.; Zhang, Z.; Xu, T.; Liu, Y.; Tu, Z.; Xu, Y.; Ren, X.; Geng, M.; Ding, J.; Pei, D. and Ding, K. Design, Synthesis and Biological Evaluation of NovelConformationally Constrained Inhibitors Targeting Epidermal Growth Factor Receptor T790M mutant. *J. Med. Chem.* **2012**, *55*, 2711-2723

39. Hughes, T.; Deininger, M.; Hochhaus, A.; Branford, S.; Radich, J.; Kaeda, J.; Baccarani, M.; Cortes, J.; Cross, N. C. P.; Druker, B. J.; Gabert, J.; Grimwade, D.; Hehlmann, R.; Kamel-Reid, S.; Lipton, J. H.; Longtine, J.; Martinelli, G.; Saglio, G.; Soverini, S.; Stock, W.; Goldman, J. M. Monitoring CML patients responding to treatment to treatment with tyrosine kinase inhibitors: Review and recommendations for harmonizing current methodology for detecting BCR-ABL transcripts and kinase domain mutations and for expressing results. *Blood* **2006**, *108*, 28-37.

40. Preuner, S.; Mitterbauer, G.; Mannhalter, C.; Herndlhofer, S.; Sperr, W. R.; Valent, P.; Lion, T. Quantiative monitoring of Bcr-Abl mutants for surveillance of subclone-evolution expansion, and depletion in chronic myeloid leukemia. *Eur. J. Cancer* **2012**, *48*, 233-236.

41. Soverini, S.; Colarossi, S.; Gnani, A.; Rosti, G.; Castagnetti, F.; Poerio, A.; Iacobucci, I.; Amabile, M.; Abruzzese, E.; Orlandi, E.; Radaelli, F.; Ciccone, F.; Tiribelli, M.; di Lorenzo, R.; Caracciolo, C.; Izzo, B.; Pane, F.; Saglio,G.; Baccarani, M.; Martinelli, G. Contribution of ABL kinase domain mutations to imatinib resistance in difference subset of Philadephia-positive patients: by the GIMEMA working party on chronic myeloid leukemia. *Clin. Cancer Res.* **2006**, *12*, 7374-7379.

42. McGinnity, D. F.; Soars, M.G.; Urbanowicz, R. A.; Riley, R. J. Evaluation of fresh and cryopreserved hepatocytes as in vitro drug metabolism tools for the prediction of metabolic clearance. *Drug Metab Dispos.* **2004**, *32*, 1247-1253.

43. Lewis, D. F. V. *Cytochromes P450: Structure, Function andMechanism;* Taylor and Francis Publishing: London, **1996**.

44. Adachi, Y.; Suzuki, H; Sugiyama, Y. Comparative studies on in vitro methods for evaluating in vivo function of MDR1 P-glycoprotein. *Pharm. Res.* **2001**, *18*, 1660–1668.

45. Giacomini, K. M.; Huang, S. M.; Tweedie, D. J.; Benet, L. Z.; Brouwer, K. L.; Chu, X.; Dahlin, A.; Evers, R.; Fischer, V.; Hillgren, K. M.; Hoffmaster, K. A.; Ishikawa, T.; Keppler, D.; Kim, R. B.; Lee, C. A.; Niemi, M.; Polli, J. W.; Sugiyama, Y.; Swaan, P. W.; Ware, J. A.; Wright, S. H.; Wah Yee, S.; Zamek-Gliszczynski, M. J.; Zhang, L. Membrane transporters in drug development. *Nat. Rev. Drug Discovery* **2010**, *9*, 215–236.

46. Branford, S.; Rudzki, Z.; Walsh, S.; Parkinson, I.; Grigg, A.; Szer, J.; Taylor, K.; Herrmann, R.; Seymour, J. F.; Arthur, C.; Joske, D.; Lynch, K.; and Hughes, T. Detection of BCR-ABL mutations in patients with CML treated with imatinib is virtually always accompanied by clinical resistance, and

mutations in the ATP phosphate-binding loop (P-loop) are associated with a poor prognosis. *Blood* **2003**, *102,* 276-83.

47. Soverini, S.; Martinelli, G.; Rosti, G.; Bassi, S.; Amabile, M.; Poerio, A.; Giannini, B.; Trabacchi, E.; Castagnetti, F.; Testoni, N.; Luatti, S.; de Vivo, A.; Cilloni, D.; Izzo, B.; Fava, M.; Abruzzese, E.; Alberti, D.; Pane, F.; Saglio, G. and Baccarani. M. ABL mutations in late chronic phase chronic myeloid leukemia patients with up-front cytogenetic resistance to imatinb are associated with a greater likelihood of progression to blast crisis and shorter survival: a study by the GIMEMA working party on chronic myeloid leukemia. *J. Clin. Oncol.* **2005**, *23*, 4100-4109.

48. Jamieson, C.; Moir, E. C.; Rankovic, Z.; Wishart, G. Medicinal Chemistry of hERG Optimizations: Highlights and Hang-Ups. *J. Med. Chem.* **2006**, *49*, 5029-5046.

49. Netzer, R.; Ebneth, A.; Bischoff, U.; Pongs, O. Screening Lead Compounds for QT Interval Prolongation. *Drug Discovery Today* **2001**, *6*, 78-84.

50. von Bubnoff, N.; Veach, D. R.; van der Kuip, H.; Aulitzky, W. E.; Säner, J.; Seipel, P.; Bornmann, W. G.; Peschel, C.; Clarkson, B. and Duyster, J. A cell-based screen for resistance of Bcr-Abl-positive leukemia identified the mutation pattern for PD166326, an alternative Abl kinase inhitor. *Blood* **2005**, 105, 1652-1659.

51. Ren, X.; Duan, L.; He, Q.; Zhang, Z.; Zhou, Y.; Wu, D.; Pan, J.; Pei, D.; and Ding, K. Identification of niclosamide as a new small-molecule inhibitior of the STAT3 signaling pathway. *ACS Med. Chem. Lett.* **2010**, *1*, 454-459.

Table of contents graphics

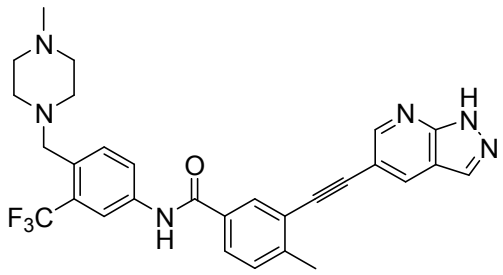

IC_{50} values:
Bcr-Abl ^{WT} 0.34 nM
Bcr-Abl ^{T315I} 0.68 nM
K562 CML cells 0.2 nM
Ku812 CML cells 0.13 nM
SUP-B15 ALL cells 2.5 nM
K_d values:
nonphosphorylated Bcr-Abl^{WT} 0.32 nM
nonphosphorylated Bcr-Abl^{T315I} 0.71 nM
phosphorylated Bcr-Abl^{WT} 0.34 nM
phosphorylated Bcr-Abl^{T315I} 3.20 nM